Very neutron-rich isotopes of light elements. Nuclear properties and production

R. Kalpakchieva and Yu. É. Penionzhkevich
Joint Institute for Nuclear Research, Dubna

H. G. Bohlen
Hahn–Meitner Institute, Berlin, Germany

Fiz. Élem. Chastits At. Yadra **29**, 832–890 (July–August 1998)

This review is devoted to the properties of neutron-rich nuclei of light elements and the problems concerning them which have been of greatest interest in recent years. The reactions used to produce such nuclei are discussed. Special attention is paid to the multinucleon transfer mechanism, used successfully for spectroscopic studies of light exotic nuclei near the neutron drip line. The feasibility of studying the structure of exotic nuclei in reactions involving radioactive beams is discussed. © *1998 American Institute of Physics.* [S1063-7796(98)00204-6]

INTRODUCTION

Light, neutron-rich nuclei are interesting for several reasons. It has been found fairly recently that they possess unusual properties. However, the main reason why they are interesting is that they may allow identification of the boundary between bound and unbound nuclei, i.e., the neutron drip line. The many existing mass formulas do not give unique information about the location of this line. The experimental determination of the neutron drip line reduces to the observation of either nuclei decaying by neutron emission, or nonobservation of a nucleus, even in the form of a resonance. Bound nuclei which live a fairly long time compared to the time for the reaction in which they are formed are called radioactive nuclei. The lifetime of a radioactive nucleus is $t > 10^{-12}$ sec. The decay of nuclei which are unstable to nucleon emission occurs relatively slowly on nuclear time scales, but fairly quickly compared to radioactive decay. The lifetimes of such nuclei lie in the range $10^{-12} > t > 10^{-22}$ sec. Nuclear states with lifetime in this range are sometimes termed quasistationary. Examples of such nuclei are ^{7}He, ^{9}He, ^{10}He, ^{10}Li, ^{13}Be, and so on. They are manifested as resonances in the cross sections for various processes. The width Γ of a resonance and the lifetime of an unstable nucleus are related as

$$T = \hbar/\Gamma = (6.6 \cdot 10^{-22})/\Gamma \text{ sec}, \quad \Gamma \text{ in MeV}.$$

Using the maximum possible time for which such a nucleus can exist, which is determined by the characteristic nuclear time ($t = 10^{-22}$ sec), the resonance width $\Gamma < 6.6$ MeV is obtained. However, only for widths $\Gamma \leq 1$ MeV is it possible to speak of a resonance as a state of a nuclear system which actually exists. The resonance energy is displaced from the threshold for this system to decay with the emission of one or more nucleons by an amount equal to the decay energy. Therefore, the observation of a resonance allows the direct determination of two important nuclear characteristics: the decay energy and the lifetime. When the lifetime is $t \sim 10^{-22}$ sec, it is assumed that the nucleus does not exist as such.

An important problem in nuclear physics is the study of the decays and properties of neutron-rich nuclei, which are either stable or unstable to nucleon emission. Any prediction of the characteristics of very neutron-rich nuclei is made by extrapolating the properties of known nuclei located in the β-stability region, assuming that these properties practically do not change with increasing number of neutrons in the nucleus. Such changes do occur rather smoothly for intermediate and heavy nuclei. However, the properties of any nuclear system are determined by the number of nucleons, and also by the interaction of only some of them. Consequently, for light nuclei even a small change in the number of nucleons can lead to a big difference in the properties of adjacent nuclei. Therefore, the extrapolation of our knowledge about nuclei near the β-stability line does not, as a rule, give any information about what to expect for nuclei far from the stability region. This is why direct experiments to study the structure of light nuclei at the drip line have always been very interesting. They have become even more interesting recently, owing to the creation of secondary beams of radioactive nuclei,[1–5] which open up new experimental possibilities.

Experiments performed in various laboratories around the world in order to study the properties of exotic nuclei with extreme values of N/Z (nuclei very far from the β-stability line) have revealed a number of unexpected phenomena: the existence of neutron and proton halos,[1,2,4–8] new deformation regions,[9,10] new types of decay, special features in the shell filling sequence,[11–19] and so on. Probably the most striking is the existence of a giant neutron halo in several light nuclei. More and more such nuclei are being discovered, and they have been found to possess completely unexpected properties which had not been predicted earlier. Therefore, experiments to study nuclei which are very neutron-rich or proton-rich are also a source of the informa-

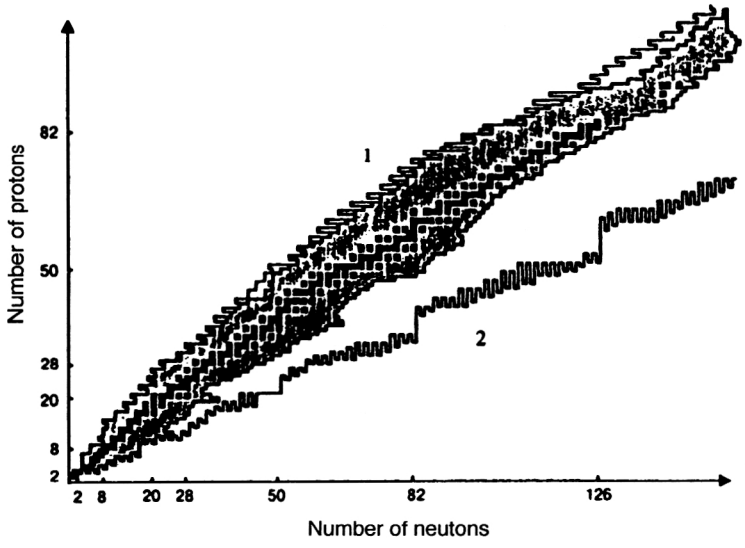

FIG. 1. Proton–neutron diagram for nuclei, showing the proton stability line (*1*) and the neutron stability line (*2*).

tion needed for testing and developing existing theoretical models.

The importance of this problem is indicated by the large number of international conferences devoted to it,[20–24] and also by the many reviews on the properties of light nuclei far from the stability line.[9,25–27] There are many publications devoted to the neutron-halo problem.[28–32] New data on the properties of very light nuclei are being obtained at a rapid rate, and so we decided that a new review is needed. In this review we attempt to describe the data obtained in the last few years on the properties of neutron-rich isotopes of light elements up to heavy isotopes of oxygen.

1. THE NUCLEAR STABILITY BOUNDARIES

1.1. The chart of the nuclides

The chart of the nuclides, shown in Fig. 1, gives the latest data on the approach to the neutron and proton drip lines. The black squares (there are about 300 of them) denote stable nuclei. They form the so-called stability valley. Nuclear stability is determined by the balance between the nuclear and Coulomb forces. The stability valley for light nuclei runs along the line $N=Z$. However, already near Ca ($Z=20$) the Coulomb forces are such that the stability line passes through the region of nuclei with a neutron excess ($N>Z$). For heavy nuclei the line corresponds to a relative neutron excess of $(N-Z)/A\approx 0.21-0.23$.

The shaded squares represent radioactive nuclei, which undergo various types of radioactive decay (α, β, p, and cluster decays or spontaneous fission). By now, 2000 such nuclei have been synthesized. This is only a small part of the ≈ 6000 isotopes whose existence is predicted theoretically.[33]

The chart also shows the calculated proton and neutron drip lines.[33] Proton instability is mainly determined by the Coulomb forces, which increase with increasing number of protons, and the lifetime of nuclei near the proton drip line is determined by the penetrability of the Coulomb and centrifugal barriers. Instability of nuclei to neutron emission is a result of the increase of the symmetry energy with increasing number of neutrons in the nucleus. The symmetry energy is given by the semiempirical nuclear mass formula:[34]

$$E_{\text{sym}}=28.1(N-Z)^2A^{-1}(1-1.18A^{-1/3}). \tag{1.1}$$

Knowing the nuclear energy $E(A,Z)$ for fixed Z, we can obtain the chemical potential of a neutron in a nucleus:

$$\mu_n(A,Z)=\left.\frac{\partial E(A,Z)}{\partial A}\right|_{Z=\text{const}} \tag{1.2}$$

Looking at E_{sym}, we see that the chemical potential μ_n is zero for a relative neutron excess $(N-Z)/A\approx 0.36$ or for $N/Z\approx 2-2.2$. This value also determines the neutron drip line.

We also see from Fig. 1 how close experimentalists have come to the neutron drip line. For example, the heaviest known isotope of calcium is ^{53}Ca, while the predicted drip line should pass near ^{65}Ca, and even ^{70}Ca is predicted to be stable. The distance between the known isotopes and the drip lines increases for heavier nuclei. For example, for tin the doubly magic isotope ^{176}Sn ($Z=50$, $N=126$) is predicted to be stable, but the heaviest isotope of tin which has so far been synthesized is ^{137}Sn. For lead isotopes, the transition from $(N-Z)/A=0.21$ (^{208}Pb) to $(N-Z)/A=0.36$ corresponds to ^{256}Pb (and the heaviest known isotope of lead is ^{214}Pb).

The situation for proton-rich nuclei is somewhat different. Here it has been possible to come very close to the proton drip line (see Fig. 1), whereas reaching the neutron drip line requires the synthesis of an enormous number of nuclei. The only exception is the region of very light nuclei (with $Z<10$), where nuclei with large neutron excess and neutron binding energy near zero have already been observed.

1.2. The neutron drip line for light nuclei

The section of the chart of the nuclides for light nuclei is shown in Fig. 2. We see that it is in this region where the largest neutron excess is attained. For example, in the ^{8}He nucleus, which is stable to neutron emission, we have the

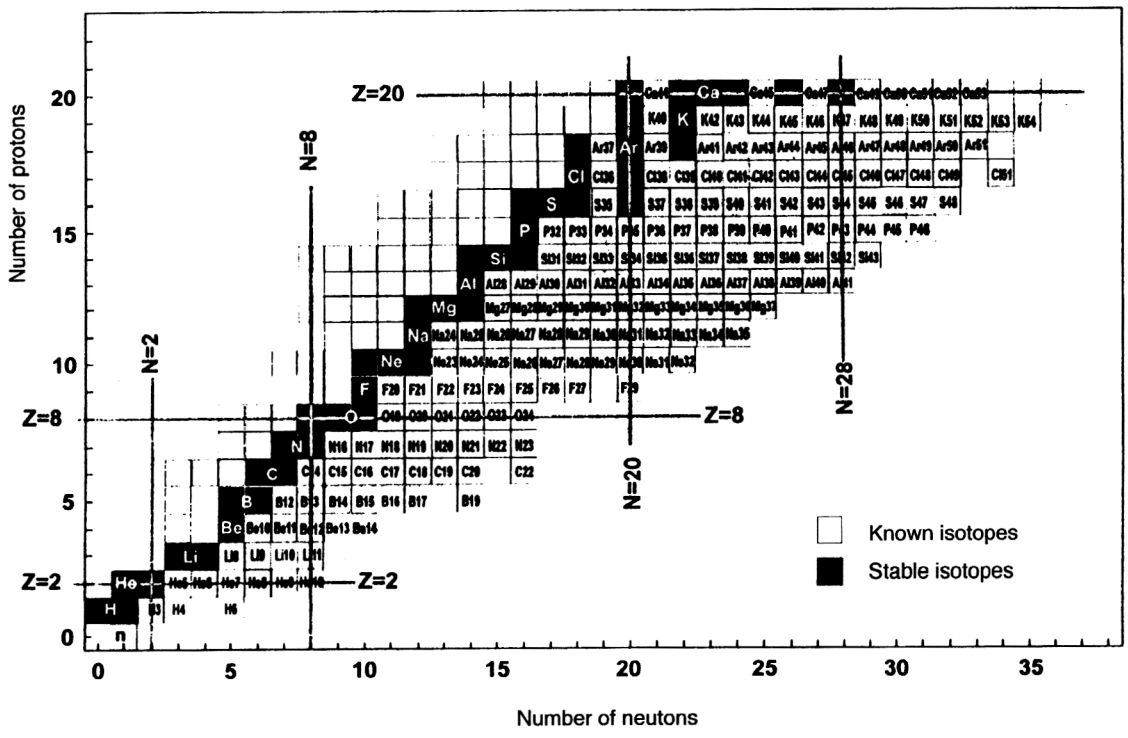

FIG. 2. Chart of the nuclides in the region of light elements.

ratio $N/Z=3$, while $(N-Z)/A=0.5$. For many light nuclei in this region the neutron excess $(N-Z)/A$ is close to or even greater than the boundary value of 0.36. At first it was thought that the neutron drip line had been reached for nuclei with atomic number $Z=4$ after the discovery of the heaviest bound isotope of beryllium, ^{14}Be (Ref. 35). Later, owing to the development of a technique for obtaining intense beams of heavy ions of intermediate and high energy, it became possible to move to larger Z. A ^{56}Fe beam was used to synthesize the heaviest bound isotope with $Z=5$, ^{19}B (Ref. 36). Later on, joint Dubna–GANIL experiments, performed at the GANIL accelerator complex using ^{40}Ar and ^{48}Ca beams at energy $\sim$50 MeV/A, not only confirmed the earlier results on the nucleon stability of ^{14}Be, ^{19}B, ^{20}C, and ^{27}F (Refs. 35–38), but also led to the discovery of the new, bound, neutron-rich nuclei ^{22}C, ^{23}N, ^{29}F, and ^{29,30,32}Ne (Refs. 39–42).

In the region of the lightest nuclei, nuclei located beyond the neutron drip line have also been discovered, i.e., nuclei which, being nucleon-unstable, live a fairly long time and appear as resonances.

There are several possible reasons why the decay of a nucleon-unstable nucleus can be delayed. The situation is different for neutron-unstable nuclei compared to proton-unstable ones, where the lifetime is fairly long, owing to the penetration of the Coulomb barrier. The stability of neutron-unstable nuclei can be affected by: (a) the isotopic-spin selection rule; (b) the existence of a centrifugal barrier (for neutrons with $\ell>0$), and (c) the need for a strong change in the initial nucleon configuration in the nuclear breakup process.

Owing to these factors, the decay rate of neutron-unstable nuclei can be decreased and their lifetime can become much larger than the characteristic nuclear time ($t \gg 10^{-22}$ sec). Only nine such nuclei are presently known (see Table I): ^{4}H, ^{6}H, ^{5}He, ^{7}He, ^{9}He, ^{10}He, ^{10}Li, ^{13}Be, and ^{16}B (Refs. 25 and 43–49). However, for a number of other nuclei, namely, ^{18}B, ^{21}C, ^{24}N, ^{25,26}O, and ^{28}F, only instability to neutron emission has been established experimentally.[36,39–42] Numerous attempts to find the nuclei ^{3}n, ^{4}n, ^{5}H, and ^{7}H have also not been successful—these nuclei have not been observed even as short-lived quantum systems, i.e., resonances.

The nucleon stability boundary is not a smooth line. This is a consequence of the effect of the neutron pairing energy on nuclear stability. In many cases the pairing energy amounts to 2–3 MeV and exceeds the binding energy of the last neutron in the nucleus, which should be manifested as an even–odd effect. This means that the addition of a single neutron to an unstable (unbound) nucleus with an odd number of neutrons significantly enhances the stability to the

TABLE I.

Nucleus	$\eta=(N-Z)/A$	Decay	Decay energy (MeV)	Width Γ (MeV)
^{4}H	0.50	^{3}H+n	3.4	$\cong$3
^{6}H	0.67	^{3}H+3n	2.7(4)	1.3(5)
^{5}He	0.20	^{4}He+n	0.89	0.60(2)
^{7}He	0.42	^{6}He+n	0.44	0.16(3)
^{9}He	0.56	^{8}He+n	1.14	$\leq$1.0
^{10}He	0.60	^{8}He+2n	1.07(7)	0.3(2)
^{10}Li	0.40	^{9}Li+n	0.24(6)	0.17
^{13}Be	0.39	^{12}Be+n	0.80(9)	$\sim$1.0
^{16}B	0.38	^{15}B+n	0.04(6)	<0.10

point of changing the sign of the binding energy. The sequence of nucleon-stable nuclei with even numbers of neutrons and nucleon-unstable nuclei with odd numbers of neutrons is thereby explained. The very long chain of boron isotopes serves as a good illustration of the experimentally observed pairing effect (^{15}B, ^{17}B, and ^{19}B with 10, 12, and 14 neutrons, respectively, are nucleon-stable, while ^{16}B and ^{18}B with 11 and 13 neutrons are unstable to neutron emission).

In view of this experimental information and its comparison with the various model predictions, it can be stated that the neutron drip line has been reached for all elements with $Z<10$. However, some authors have suggested that in principle there can be a number of factors which cause the neutron drip line not to exist at all or which allow the existence of "islands of stability" far beyond the drip line, where N/Z is very large.[25,30,50] This is suggested by the systematics of the one- and two-neutron binding energies,[47] which indicate that, for some heavy isotopes of light elements near the drip line, these energies fall off smoothly with increasing mass number and approach the value $B_{n,2n}=0$ nearly tangentially. Moreover, as this occurs for nuclei with a two-particle halo, it may turn out that neutron clusters containing a larger number of neutrons can be bound to the core and form even heavier weakly bound systems.

Thus, the exact determination of the drip lines for both neutrons and protons is an important but very complicated theoretical problem. This is because the parameters of the mass formulas are determined by extrapolating nuclear properties known near the β-stability line to the region of nuclei with much larger N/Z. It is well known that different models give contradictory results for the same nucleus; sometimes the predicted binding energies of the last nucleons added to the nucleus differ by 5 or more MeV, and so the stability of these nuclei can be predicted only with this accuracy. As a result, the location of the nucleon stability line is model-dependent. A detailed analysis[33] of the various mass calculations has shown that they can differ strongly in predicting whether or not a given nucleus is stable. Accordingly, the drip lines predicted by various models can differ by several isotopes. Therefore, only experiment can tell whether or not nuclei with a large neutron excess are stable and what their structure is. In this sense, any new experimental result for a nucleus with an unusual value of N/Z is an important test of the existing theoretical models.

Let us give a few examples. The nuclei ^{14}Be and ^{29}Ne have been observed experimentally,[35,39] although their instability to nucleon emission had been predicted earlier by various models. An experiment using a ^{48}Ca beam (44 MeV/A) did not reveal the isotope ^{26}O, but the heaviest nucleon-stable isotope of neon, ^{32}Ne, was synthesized,[42] which contradicts the predictions of various mass formulas.[33] It should be noted that the nonobservation of a nucleus in an experiment cannot unambiguously indicate whether or not that nucleus is nucleon-stable. This is illustrated by ^{14}Be and also ^{31}Ne, which were not observed in early experiments,[42,51] but were unambiguously identified in later experiments using other reactions.[35,39,42,52,53]

Special cases of the problem of determining the location of the neutron drip line are searches for the possible existence of islands of nucleon-stable nuclei located far beyond the predicted drip line, and also for the possible existence of nuclei consisting only of neutrons.

The available experimental data indicate that only for the lightest elements ($Z<10$) is it possible to arrive at definitive conclusions about the location of the neutron drip line. It is difficult to say anything definite about the location of this line for nuclei with $Z\geqslant 10$. The heaviest neutron-rich nuclei with $10\leqslant Z\leqslant 13$ have recently been discovered: ^{32}Ne (Ref. 42), ^{39}Al (Ref. 41), and also ^{31}Ne, ^{37,38}Mg, and ^{40,41}Al, in reactions involving ^{50}Ti and ^{48}Ca ions.[52,53] The latter studies confirm that the exact determination of the neutron drip line continues to be one of the most important problems of nuclear physics.

2. WHY ARE LIGHT, NEUTRON-RICH NUCLEI INTERESTING?

The synthesis and study of neutron-rich isotopes have two fundamental goals: determining the location of the neutron drip line and obtaining information about the properties of exotic nuclei near this line. Owing to progress in accelerator technology, it has become possible to obtain accelerated beams of secondary radioactive nuclei, and this has opened up broad new possibilities in the study of both the structure of the lightest exotic nuclei and the nuclear interactions in which these nuclei participate.

It is extremely important to obtain new information about nuclei located near the nucleon stability boundary, since it can be expected, and has already been experimentally observed, that the properties of these nuclei differ significantly from the usual nuclear properties. It is convenient to study nuclei with small Z. However, the fundamental question arises of how general are the conclusions drawn on the basis of such a small number of nuclei. Again, this can only be answered by experiment.

2.1. The nuclear mass

A fundamental characteristic of a nucleus is its mass. The experimental determination of the mass is one of the necessary conditions for determining the stability and properties of weakly bound nuclei. The measured mass is used to determine the nuclear binding energy, which reflects the balance between the nuclear and Coulomb forces and, therefore, the nucleon configuration. Nuclear mass measurements also give direct information about the stability boundaries. For a number of nuclei, for example, ^{8,9,10}He, ^{11}Li, ^{14}Be, and ^{16}B, experiment has not only shown that they are bound (^{9,10}He and ^{16}B), but also that some of them are completely stable (^{8}He, ^{11}Li, and ^{14}Be).

Measurement of the masses of helium isotopes revealed the so-called helium anomaly.[54] It had been found that the larger the number of neutrons in the nucleus, the lower the binding energy of the last neutron. Of course, as shown above, owing to nucleon pairing this dependence must be studied separately for nuclei with even and odd numbers of neutrons. The monotonic dependence of the binding energy is modified by shell effects. The stability is decreased by the

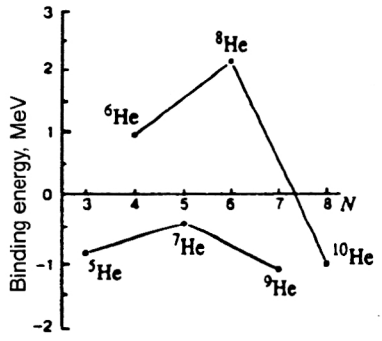

FIG. 3. Binding energy of one and two neutrons in He isotopes (the helium anomaly).

addition of two neutrons for practically all the known nuclei of light elements. It was found that an exception to this rule is the pair of nuclei ^{15}N, ^{17}N, for which the stability is increased beyond the experimental error. Isotopes of He were the next exception discovered. The largest increase of stability with increasing number of neutrons is observed for the pair ^{6}He, ^{8}He, for which the increase is about 1 MeV. The binding energy also increases in going from ^{5}He to ^{7}He. Going from ^{5}He to ^{9}He (i.e., increasing the mass number by four neutrons) practically does not change the binding energy. The isotope ^{10}He turned out to be considerably more stable than predicted ($E_{2n}=1.07-1.2$ MeV; Refs. 43 and 44). This effect is referred to as the helium anomaly (Fig. 3). There is not yet any good explanation of this unusual behavior of the binding energy in these nuclei. However, it has been suggested that it is related either to the large neutron excess in these nuclei, or to the effect of the centrifugal barrier on the stability. Further data on the masses of very neutron-rich isotope pairs are needed to understand such anomalies.

Measurement of the nuclear masses also gives information about the evolution of the nuclear shape. This is discussed in Sec. 2.3 below.

2.2. The nuclear level scheme

The level schemes of light, neutron-rich nuclei which are either stable or unstable to decay with neutron emission are also of great interest. Until recently, information about the levels was rather sparse, and even the fact that excited states exist had not been established. For example, the presence of excited levels for the heaviest stable isotopes ^{3}H, ^{8}He, ^{11}Li, and ^{14}Be and for the unstable isotopes ^{10}He, ^{10}Li, and ^{16}B was discovered only recently. Experimental data on the levels and their quantum characteristics allows the determination of the level-filling sequence and thus the applicability of any particular theoretical model, the presence of a collective excitation (for example, a soft dipole mode), the type of decays that the levels undergo, and so on. These questions will be studied in more detail later in this review.

2.3. The nuclear shape

In theoretical studies it has been argued that a deformation can tend to increase the nuclear binding energy. From this point of view nuclei with $N=20$ neutrons are particularly interesting, as their ground state is expected to be spherical, owing to the filling of the closed shell with $N=20$. However, recent theoretical calculations of their binding energies predict a strong longitudinal deformation $\beta \approx 0.3$ for some of them, and even the existence of isomer states. It is assumed that, as a consequence of this deformation, one should experimentally observe a sharp increase of the two-neutron binding energy in the neutron-rich nuclei ^{31}Na and ^{32}Mg, i.e., inversion of the Nilsson levels corresponding to large deformation.[55–57] This result, which indicates that the closed shell is violated and that $N=20$ is not a magic number, was unexpected. Later experiments were performed using ^{33,34,35}Al, ^{35}Si, and ^{36,37}P nuclei (Refs. 58 and 59) to determine the region where this deformation appears. However, they did not reveal any deviations of the two-neutron binding energy from the shell-model calculations, and it was concluded that nuclei with $Z \geqslant 13$ and $N=20$ are spherical, and that for them $N=20$ corresponds to a normal, closed, spherical shell. However, these conclusions are not definitive, because recent experiments on the measurement of $T_{1/2}$ for ^{27,29}F and ^{30}Ne have shown that these nuclei are also more stable than predicted by the shell model.[60] The recently measured[10] large value of the reduced transition probability $B(E2;0^{+}\rightarrow 2^{+})$ for ^{32}Mg ($N=20$) also confirms the possible existence of such a deformation in light nuclei. Moreover, the experimental discovery of the very neutron-rich isotopes ^{31}Ne and ^{37}Mg (Ref. 52) agrees with the theoretical calculations predicting the stability of these isotopes when deformation is included.

Finally, let us consider the isotope ^{28}O. This doubly magic ($N=20$, $Z=8$) nucleus has not yet been observed experimentally. However, the nucleus ^{29}F with the same number of neutrons but one more proton ($N=20$, $Z=9$) has proved to be nucleon-stable. If this stability is not a consequence of the pn interaction, it can be assumed that the deformation effect in ^{29}F is stronger than in ^{31,32}Na, which explains the stability. Further study of the properties of nuclei near $N=20$ is necessary.

2.4. Nuclear sizes

The determination of nuclear sizes has always been a fundamental topic of nuclear physics, since for many calculations it is necessary to have accurate values of the nuclear matter distribution. These distributions have been studied primarily in experiments on electron scattering (which give information about the nuclear charge distribution) and hadron scattering (which give information about the nucleon distribution in the nucleus).[61]

With the appearance of secondary radioactive beams it became possible to extend considerably the range of nuclei for which the nuclear size can be determined from measurements of the cross sections for reactions induced by these nuclei. It has long been known[62] that, in principle, changes in the binding energy are correlated with the nuclear size. However, the results for light nuclei exceeded all expectations. A number of new, interesting features were discovered which are related exclusively to the small binding energy of the

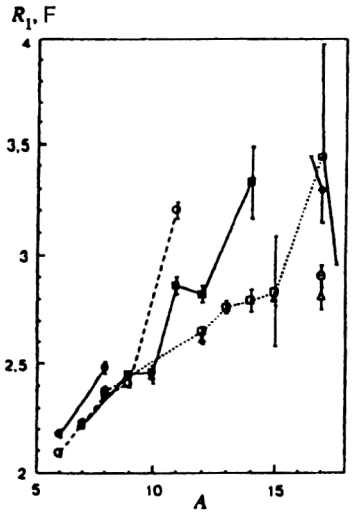

FIG. 4. Interaction radii of light nuclei extracted from the experimental values of the interaction cross sections.[1–3, 63–67] The data are for He (●), Li (○), Be (■), B (□), C (▲), N (⊙), F (△), and Ne (◇).

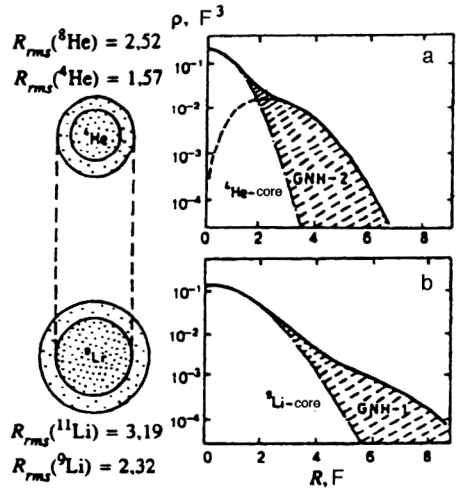

FIG. 5. Neutron density distribution in ^{8}He (a) and ^{11}Li(b).

valence neutrons in nuclei located at the neutron drip line. For example, in reactions involving secondary radioactive beams of He, Li, Be, and B isotopes it was found that the reaction cross section for several isotopes is exceptionally large.[1] The radii of the nuclear matter distributions obtained in these experiments display a gradual increase with increasing number of neutrons, while for the nuclei ^{11}Li, ^{11}Be, ^{14}Be, and ^{17}B, which are close to the drip line and weakly bound, these radii significantly exceed the values given by the dependence $\sim A^{1/3}$ (see Fig. 4).[1–3,63–67]

At present such studies are being extended to heavier elements, as can be seen, for example, from Ref. 68.

The determination of the regularities in the behavior of the radii as a function of the mass, isospin, and energy in a wide range of values makes it possible to discover new nuclei with a neutron halo. Here the study of mirror nuclei, in which one of the nuclei is unbound, is particularly informative. The measured values of the quadrupole moments and also the differences in the Coulomb energy can be used to derive a new type of systematics in seeking unusual states of exotic nuclei. The systematics of all seven pairs of mirror nuclei has confirmed the existence of a neutron halo in the isotopes ^{6}He and ^{8}He. It also predicts a halo in the nuclei ^{9}Be and ^{15}C ($R_n^{\rm rms}-R_p^{\rm rms}\approx 0.20-0.30$ F) and indicates inversion of the s and d orbits in the mirror pair ^{17}Ne, ^{17}N (Ref. 69).

2.5. The neutron halo

The anomalous increase of the radius of very neutron-rich nuclei has been interpreted as a manifestation of a neutron halo in these nuclei, where the valence neutrons in a weakly bound nucleus form a long tail in the neutron density distribution.[6] The halo is a characteristic of a bound state lying near the particle emission threshold. It is specific to light, very neutron-rich nuclei and had not been observed earlier. Subsequent experiments using fragmentation reactions and dissociation in the field of the target nucleus, and also measurement of the nucleon or fragment momentum distributions resulting from collisions, confirmed the assumption that a neutron halo exists in nuclei (Refs. 4, 5, 28, 29, 65, and 70–84).

Thus, increase of the radius was the first sign of a halo in exotic nuclei. However, later on two types of halo were found.[85] The first was associated with an overall increase of the nuclear size (for the nuclei ^{11}Li, ^{11}Be, ^{14}Be, and ^{17}B). The second occurs in nuclei of normal size (for example, ^{6}He and ^{8}He). The difference between them is illustrated in Fig. 5 for ^{11}Li and ^{8}He. It is assumed that the first type of halo arises owing to very small binding energy of the valence neutrons, while the second type of halo is the result of the very compact (α-particle) core of the ^{6}He and ^{8}He nuclei. In Ref. 86 the interaction and fragmentation cross sections for the nuclei ^{4,6,8}He were measured at energy 800 MeV/A, and it was concluded that the increase of the interaction cross section with increasing mass number is associated with the cross section for neutron stripping. By determining the neutron and proton spatial distributions, it was found that $R_n^{\rm rms}-R_p^{\rm rms}\approx 0.9$ F for ^{6}He and ^{8}He. This extension of the neutron distribution relative to the proton one is referred to as the neutron skin. The existence of the neutron skin in ^{8}He was also confirmed in Ref. 87. There is no clear distinction between a neutron skin and a neutron halo, although these concepts can distinguish between the cases of very low and relatively large binding energies of the last neutrons [for example, $S_{2n}(^{11}\text{Li})\approx 0.3$ MeV and $S_{2n}(^{11}\text{Be})=0.5$ MeV versus $S_{2n}(^6\text{He})=0.97$ MeV and $S_{2n}(^8\text{He})=2.14$ MeV; Ref. 86].

It has been suggested that two-neutron halos in the form of a dineutron exist. This question is as important as that of correlations between the neutrons of the halo and the nuclear core.

There are several reviews (Refs. 26, 27, 29–32, and 88–91) which not only give the facts, but also trace the development of the understanding of the neutron halo. We will return to this problem later on.

It follows from our discussion that the new phenomena discovered recently in studying the properties of very light nuclei at the neutron drip line have made it necessary to

review many of the ideas about these nuclei. There are a number of open questions which should be answered experimentally in the very near future:

• First, there is the level structure of nuclei with a neutron halo. A new type of collective excitation at low excitation energies[5,92,93] has been proposed to explain the increased cross section for the electromagnetic dissociation of such nuclei. This new excitation mode is referred to as the soft dipole resonance. The existence of a low-energy $E1$ dipole has now been confirmed for several nuclei,[28,82,94–97] but the mechanism for exciting it has not yet been uniquely explained. Nevertheless, the value of the excitation energy is model-dependent.[93] It is also necessary to search for predicted excitations of higher multipole order.

• Data on new, heavier nuclei with a halo are needed, since so far only a few nuclei with a 2-neutron halo (^{6}He, ^{8}He, ^{11}Li, ^{14}Be, and ^{17}B) and only two with a 1-neutron halo (^{11}Be and ^{19}C) are known.[98] The existence of many nuclei with a halo is predicted. It is largely the advent of radioactive beams which has made the formation and study of such nuclei possible.

• Another interesting question is that of the shell-filling sequence.[11,15–19,99–101] It is also necessary to determine the N and Z at which shells are closed, and how pairing and shells, including deformed ones, affect nuclear stability.

• The question of nuclear sizes is extremely important. The use of secondary radioactive beams allows the isospin dependence of the spatial distribution of nuclear matter to be determined for many exotic nuclei.

• The question of correlations between the nucleons of the neutron halo remains unanswered. The fragmentation of exotic nuclei in the form of beams is the best way of studying the correlations between their components. It is expected that practically kinematically complete experiments of the type in Refs. 82 and 94 will give an answer.

• Do nuclei with a halo contain a dineutron?

The experimental resolution of these and several other problems for light, neutron-rich nuclei is related to the possibility of obtaining sufficiently large quantities of exotic nuclei. In the following section we shall discuss the known methods of obtaining light nuclei near the neutron drip line.

3. OBTAINING NEUTRON-RICH ISOTOPES OF LIGHT ELEMENTS

3.1. The fission reaction

Spontaneous nuclear fission is accompanied by the emission of light charged particles formed at the moment when a heavy nucleus splits into two fragments. There is a large probability that these light charged particles are neutron-rich. Neutron-rich isotopes of H, He, Li, Be, and even heavier elements have been observed in the spontaneous fission of ^{252}Cf (Refs. 102 and 103). Exotic nuclei like ^{10}He and ^{7}H have also been sought in the spontaneous fission of ^{252}Cf (Refs. 104–106). In Refs. 104 and 106 no events were found which could be attributed to ^{10}He. The upper limit on the emission of ^{10}He relative to ^{8}He was found to be $Y(^{10}\text{He})/Y(^{8}\text{He}) \leq 4\times10^{-3}$. Meanwhile, in Ref. 105 the authors think that several events corresponding to ^{10}He were observed. The experiment of Ref. 106 gave the ratio $Y(^{7}\text{H})/Y(^{3}\text{H}) \leq 1\times10^{-4}$ for ^{7}H.

Fission induced by thermal neutrons has been used to synthesize exotic neutron-rich nuclei with $A=60–160$ (see, for example, Ref. 107). Experiments on fission induced by ^{40}Ca and ^{48}Ca ions[108] have shown that a strong neutron excess of the bombarding ion can lead to the synthesis of nuclei farther from the β-stability line. It has also been shown that fission induced by protons[109] and heavier ions[110,111] leads to an increase of the probability for triple fission with the emission of light particles and nuclei. This is the result of the higher excitation energy and the higher angular momentum of the fissioning nucleus. However, the high excitation energy transferred to the fragments makes it necessary for them to evaporate neutrons, thereby decreasing the probability of forming neutron-rich nuclei.

3.2. Fragmentation of the target nucleus

Target-nucleus fragmentation reactions are effective for synthesizing neutron-rich nuclei if protons with energy of several GeV and higher and targets with $Z>80$ are used. The location of the maximum of the isotopic distribution of the products depends on the target mass. As N/Z of the target increases, N/Z of the products of the fragmentation reaction also grows.

During the 1960s and 70s high-energy proton accelerators made it possible to use such reactions to search for new nuclei. For example, the nuclei ^{11}Li, ^{14}B, ^{15}B, ^{17}C, ^{19}C, ^{19}N, and ^{21}O were first synthesized at that time.[112,113]

From the systematics[114] of the cross sections for the production of neutron-rich nuclei in target-fragmentation reactions it can be concluded that the probability of producing nuclei with extreme values of the neutron excess is very large. The cross sections for producing several nuclear systems were estimated in Ref. 115: $\sigma(^{8}n)\approx10^{-30}$ cm^2, $\sigma(^{10}\text{He})\approx10^{-29}$ cm^2, and $\sigma(^{13}\text{Li})\approx10^{-30}$ cm^2.

However, when intense beams of heavy ions became available it became possible to use heavy-ion reactions for this research. In the following sections we discuss the wide range of heavy-ion reactions used to study exotic nuclei.

3.3. Deep-inelastic transfer reactions

In the late 1960s, the use of transfer reactions induced by the heavy ions ^{11}B, ^{15}N, ^{18}O, ^{22}Ne, and ^{40}Ar led to the synthesis of about 30 new isotopes of carbon, nitrogen, oxygen, fluorine, neon, magnesium, aluminum, silicon, phosphorous, sulfur, and chlorine.[116,117] Much later, the same mechanism with ^{40}Ar and ^{56}Fe beams was used to obtain even more neutron-rich isotopes of elements with $Z=14–26$ (Refs. 118–120).

The first indication that a mass transfer of nucleons accompanied by a significant loss of kinetic energy can occur in the interaction of two complex nuclei was obtained at Dubna[121] already in the late 1960s. Further experimental and theoretical studies in this area revealed several regularities in the formation of products of deep-inelastic transfer reactions, on the basis of which it was concluded that such reactions

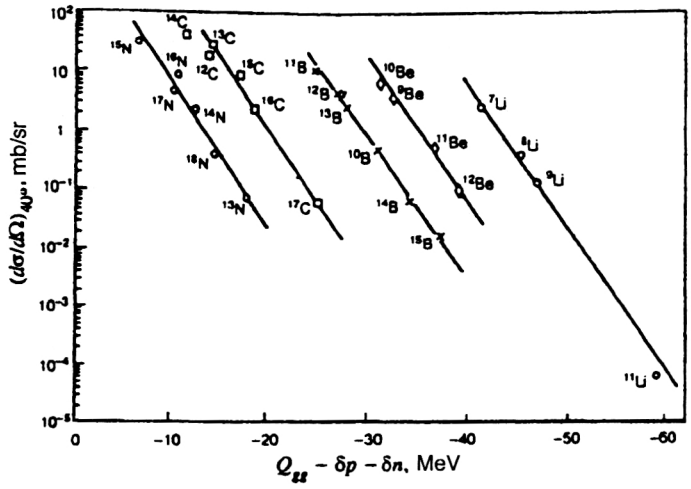

FIG. 6. Q_{gg} systematics of the production cross sections for transfer reactions in the system ^{232}Th+^{16}O (137 MeV) (Refs. 122 and 123).

can be a useful method of synthesizing new nuclei, including neutron-rich isotopes of light elements. It is very important to know how the cross section for isotope production varies with increasing distance of the isotope from the β-stability line. A method of describing the dependence of the isotope-production cross section on the number of neutrons using the Q_{gg} systematics was suggested in Refs. 122 and 123. According to this systematics, the cross sections for isotope production lie on a line whose slope is the same for all isotopes of a given element produced in a given reaction (see Fig. 6). The Q_{gg} systematics can therefore be used to extrapolate the cross sections for the production of unknown isotopes. However, the accuracy of this extrapolation is determined by the accuracy with which the masses are determined by various mass formulas, since Q_{gg} depends on the difference of the nuclear masses in the initial and final channels: $Q_{gg}=(M_1+M_2)-(M_3+M_4)$. Taking into account the statistical nature of deep-inelastic transfer reactions and making corrections for proton and neutron pairing, the isotope-production cross section is given by[122]

$$\sigma=\exp[(Q_{gg}+\Delta E_C+\Delta E_{rot}-\delta(p)-\delta(n))/T], \quad (3.1)$$

where ΔE_C and ΔE_{rot} are the changes in the Coulomb and rotational energies of the system, $\delta(p)$ and $\delta(n)$ are the pairing corrections, and T is the temperature of the binary nuclear system. This dependence is used successfully to describe the experimental regularities in the probabilities for isotope production in deep-inelastic transfer reactions.

However, the situation is different when we deal with nuclei near the neutron drip line. For example, the cross sections for producing ^{11}Li and ^{14}Be turned out to be much smaller than predicted by the Q_{gg} systematics, and only an upper limit was obtained for ^{10}He production, which turned out to be two orders of magnitude lower than expected.[124] These deviations from the Q_{gg} systematics might be related to the fact that all these nuclei are very weakly bound. The possibility of using deep-inelastic transfer reactions to synthesize nuclei at the nucleon drip line therefore remains open (although such reactions have proved very effective for synthesizing nuclei which are not so exotic).

3.4. Heavy-ion reactions accompanied by the emission of fast, light, charged particles

In the late 1970s and 1980s physicists were attracted to these reactions, owing to the unusual mechanism for fast-particle production. Already in 1961 it had been observed[125] that there are two components in the distribution of α particles produced in heavy-ion reactions. One of these components is evaporation α particles, and the other is high-energy particles with angular distributions strongly peaked in the forward direction and with maximum yield at the energy corresponding to the velocity of the bombarding ion.

Later experiments showed that in reactions involving ions heavier than ^{12}C, the cross section for the emission of heavier charged particles is fairly large.[126] A phenomenological model based on the assumption that a part of the incident ion is transferred to the target nucleus while the rest travels in the forward direction gives a fairly good reproduction of the cross section for the production of isotopes with $Z=1-4$. Meanwhile, other characteristics of the process cannot be explained within any one particular model.[127] We see from Fig. 7 that the energy spectra of different particles fall off exponentially with increasing particle energy until the energy differs by only a few MeV from the maximum possible value allowed by energy and momentum conservation for the two-body reaction mechanism.[126,128] When the particle energy is equal to the energy at the kinematical limit, the two nuclei produced in the exit channel are in the ground state. The difference observed between the experimental and calculated limiting energies is determined by the angular momentum of the residual heavy nucleus, which depends on the energy of the bombarding ion and on the type of emitted particle. For example, in the emission of Be nuclei the energy reaches the kinematical limit with relatively large cross section ($\sim 10^{-30}$ cm^2/MeV·sr). The observed effect suggests that reactions with fast-particle emission can be used to synthesize exotic nuclei. Attempts to synthesize exotic nuclei like ^{10}He, ^{14}Be, and so on have been made using these reactions.

Searches for ^{10}He have been carried out[124] using the reaction ^{232}Th+^{11}B (89 MeV). This reaction was selected from

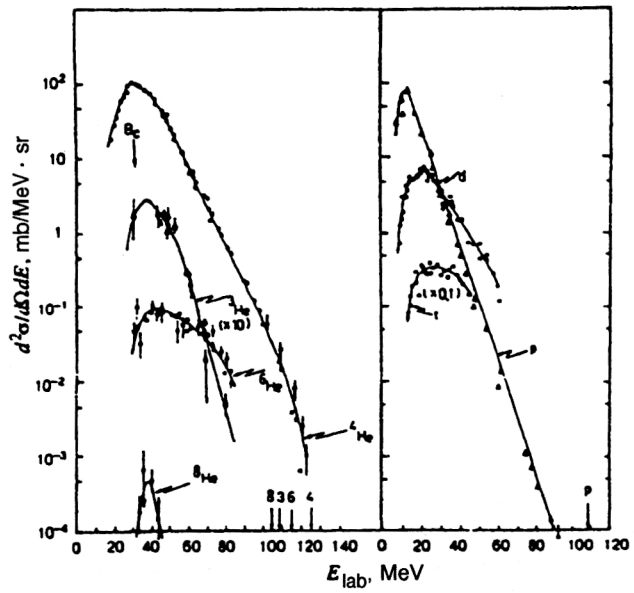

FIG. 7. Energy spectra of H and He isotopes measured in the reaction ^{232}Th+^{22}Ne (178 MeV) at the angle 0°. The arrow labeled B_C indicates the Coulomb barrier in the exit channel. The arrows on the E_{lab} axis indicate the kinematical limits for various particles.[126]

among several others because the yield of light charged particles (in particular, the isotope ^{8}He) in it is much larger than in other reactions. The energy spectra of helium isotopes measured in this experiment are shown in Fig. 8. Extrapolation of the cross sections for the production of known nucleon-stable isotopes of helium gave the expected value of the cross section for ^{10}He production in this reaction: $\sim 5 \times 10^{-30}$ cm^2/sr (Fig. 9). However, the upper limit on

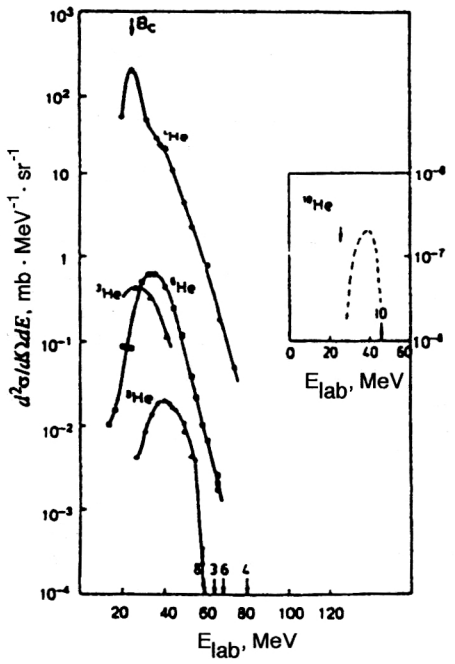

FIG. 8. Energy spectra of He isotopes measured in the reaction ^{232}Th+^{11}B (89 MeV) at 20°. The arrows are the same as in Fig. 7. The insert shows the proposed shape of the energy spectrum of the ^{10}He nucleus.[124]

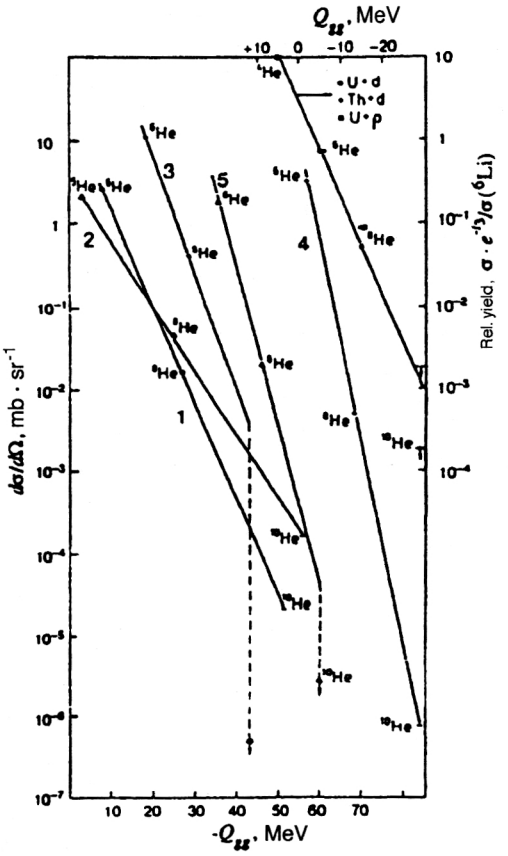

FIG. 9. Dependence of the yields of helium isotopes on the Q value of the reaction for reactions involving deuterons, protons, and the heavy ions ^{15}N, ^{22}Ne, and ^{10,11}B (Ref. 124). The reactions are ^{nat}Ti+^{22}Ne(0°) (*1*), ^{nat}Ti+^{10}B(20°) (*2*), ^{232}Th+^{11}B(20°) (*3*), ^{232}Th+^{22}Ne(0°) (*4*), and ^{232}Th+^{15}N(40°) (*5*).

^{10}He production obtained experimentally is only $\sim 5 \times 10^{-34}$ cm^2/sr. This result indicates that ^{10}He is unstable.

3.5. Reactions with fragmentation of the bombarding ion

Reactions of this type have been used to synthesize and study the properties of exotic nuclei from the time it became possible to accelerate heavy ions to energies $E > 40$ MeV/A.

Early experiments using ^{12}C, ^{14}N, ^{16}O, and ^{20}Ne beams at energies of 1–2 GeV/A have shown that relativistic collisions between complex nuclei lead to the production of nuclei far from the stability line.[129]

The first studies on the synthesis of new nuclei were performed using ^{40}Ar and ^{48}Ca beams with energy ~ 200 MeV/A, and then about 15 new exotic nuclei ranging from N to Cl were synthesized.[130,131]

It turned out that fragmentation reactions possess important characteristics which make them convenient for obtaining exotic nuclei. First, products in a wide range of A and Z are formed in these reactions. Second, the product velocities practically coincide with the incident ion velocity. Third, owing to the large velocity transfer, the products have angular distributions strongly peaked in the forward direction. Finally, the ratio N/Z in the products is sensitive to the ratio

in the bombarding ion. In fact, experiments have shown that the yield of, for example, neutron-rich isotopes of Na in reactions involving ^{48}Ca ions is much higher than that in reactions involving ^{40}Ar ions.[130,131] Therefore, for the synthesis of neutron-rich nuclei it is preferable to use beams of ions such as ^{36}S, ^{48}Ca, ^{58}Fe, and so on. The calculations performed in Ref. 132 confirm this: the isotopic distributions are strongly correlated with the ratio N/Z in the bombarding ion. In Ref. 37 a ^{48}Ca beam was used to synthesize the new isotope ^{27}F. The heaviest isotope of boron, ^{19}B, was observed[36] in a ^{56}Fe beam (670 MeV/A). This isotope was obtained as a result of stripping 37 nucleons (21 protons and 16 neutrons) from the bombarding ion!

Later on, joint Dubna–GANIL experiments using fragmentation reactions at intermediate energies ($E \geqslant 35$ MeV/A) for ^{40}Ar, ^{48}Ca, and ^{86}Kr beams obtained a large number of neutron-rich isotopes of C, N, F, Ne, Ar, Ti, V, Cr, Mn, Fe, and Co.[39–42,133]

Quite recently, at RIKEN in Japan beams of ^{50}Ti ions of energy 80 MeV/A were used to synthesize the two new neutron-rich isotopes ^{31}Ne and ^{37}Mg (Ref. 52), and the joint Dubna–RIKEN experiment using a ^{48}Ca beam of energy 70 MeV/A was the first to observe the new isotopes ^{38}Mg and ^{40,41}Al (Ref. 53). These experiments also show that the use of beams of neutron-rich nuclei, with the other conditions unchanged, leads to an increase of 1 to 2 orders of magnitude in the cross section for producing new isotopes in reactions with fragmentation of the bombarding ion.

Here we should emphasize the special role played by reactions with fragmentation of the bombarding ion in obtaining secondary beams. The special features of these reactions, namely, the strong forward peaking of the angular distribution and the closeness of the product velocities and the ion velocity, i.e., the small momentum spread, have made it possible to collect these products to form secondary beams of radioactive nuclei from them. This new area in nuclear physics has developed in the last 10 years. Reactions involving radioactive beams have been used to obtain information on nuclear structure by measuring experimental quantities like the reaction cross section, the momentum distributions, and the correlations between the products of the breakup reaction. This has led to important discoveries like the existence of a neutron halo in ^{11}Li (Refs. 1–6), ^{10}He in reactions involving ^{11}Li beams,[43] and so on. Therefore, the use of secondary beams is very promising for studies on exotic nuclei.

3.6. Charge-exchange reactions

Charge-exchange reactions involve the replacement of one or more protons by one or more neutrons. The simplest reactions of this type are (p,n) and (n,p) reactions. Although the nuclear charge is changed, the mass number remains the same.

Double charge-exchange reactions induced by π mesons, (π^-,π^+), occupy a special place in searches for exotic nuclei such as $4n$, ^{5}H, ^{6}H, ^{7}H, and ^{9}He (Refs. 134–136). The ^{11}B$(\pi^-,\pi^+)^{11}$Li reaction was used to accurately determine the ^{11}Li mass, and an excited level at energy $E^* = 1.2 \pm 0.1$ MeV was observed. It was interpreted as the discovery of a soft dipole resonance in this nucleus.[28] Measurement of the ^{9}He mass and determination of its levels in π-meson reactions[136] have shown that ^{10}He may be more stable than expected on the basis of various models. This was a factor which stimulated the experiments to search for ^{10}He.

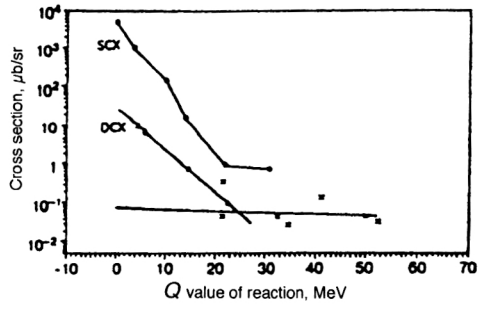

FIG. 10. Systematics of the known cross sections for single (SCX) and double (DCX) charge-exchange reactions obtained in heavy-ion beams and leading to the production of final nuclei in the ground state.

Charge-exchange reactions have large cross sections also when heavy ions are used. The first studies using double charge exchange on heavy ions[137,138] showed that the reaction cross section grows with the energy of the bombarding ion and that the angular distributions are peaked in the forward direction. It was also shown[139,140] that nuclei in the ground state are produced in charge-exchange reactions. In Fig. 10 we show the systematics of the known cross sections for single and double charge exchange leading to the production of final nuclei in the ground state. It can be concluded that these cross sections are correlated with the Q value of the reaction. The experimental points up to Q values of about -20 MeV were obtained for beam energies of up to 10–15 MeV/nucleon, and the results at more negative Q were obtained for beam energies of 25–35 MeV/A. In addition to the Q value, the charge-exchange cross section depends on the energy of the bombarding ion. This was the conclusion of Refs. 137, 141, and 142, in which the effect of the energy of the bombarding ion on the charge-exchange mechanism was studied to see whether the latter was direct charge exchange or sequential replacement of proton(s) by neutron(s). The mechanism for this reaction depends not only on the energy, but also on the levels which are populated. The structure of the interacting nuclei also has an important effect. It has been shown[143] for the reactions (^{12}C, ^{12}N), (^{12}C, ^{12}B), (^{13}C, ^{13}N), and (^{13}C, ^{13}B) that charge-exchange reactions are highly selective. By choosing a suitable target–bombarding-ion combination, it is possible to populate different final states with larger or smaller cross sections. For example, the reaction (^{12}C, ^{12}N) is dominated by the population of states with $\Delta S = 1$, i.e., states with unnatural parity, whereas the reaction (^{13}C, ^{13}N), where $\Delta S = 0$, is dominated by non-spin-flip transitions. In the reaction (^{13}C, ^{13}B) there are two types of level population, but transitions with $\Delta S = 1$ are more likely (Fig. 11).

Since the cross sections for charge exchange on heavy ions are relatively large and these reactions are selective in populating particular levels, it has been concluded that they can be used to synthesize nuclei near the nucleon stability

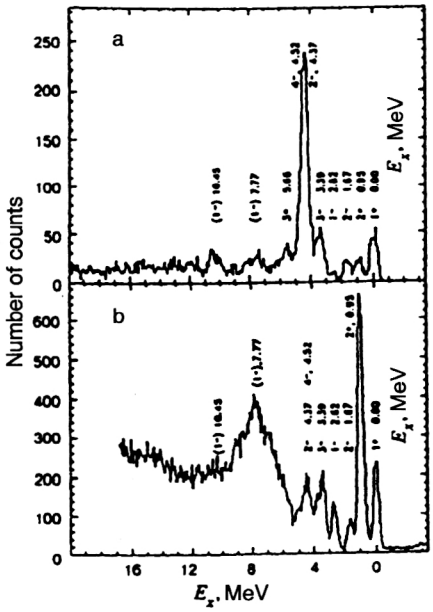

FIG. 11. Energy spectra obtained in (^{12}C, ^{12}N) and (^{13}C, ^{13}N) reactions on a ^{12}C target at beam energy 30 MeV/A (Ref. 143). For the first reaction (a) E_{lab}=358.4 MeV, θ_{lab}=3.4°, $\Delta\theta$=0.6°; for the second reaction (b) E_{lab} =379.1 MeV, θ_{lab}=0°, $\Delta\theta$=4°.

line. For example, the nucleus ^{9}He has been studied in ^{9}Be(^{13}C, ^{13}O)^{9}He and ^{9}Be(^{14}C, ^{14}O)^{9}He reactions.[144,145] The cross section obtained for the production of ^{9}He in the ground state turned out to be about 40 nb/sr. The nucleus ^{13}Be has been studied[146] in the (^{14}C, ^{14}O) reaction on a ^{13}C target, and ^{11}Li has been studied[147] in the ^{14}C(^{11}B, ^{11}Li) reaction. The double charge-exchange reaction ^{10}Be(^{14}C, ^{14}O)^{10}He has recently been used to determine the ^{10}He mass, and two excited levels were found.[44] The cross section for ^{10}He production in this reaction was found to be 140 nb/sr.

Thus, charge-exchange reactions on heavy ions are a good tool for studying exotic nuclei. It should again be noted that under certain conditions the mechanism for these reactions can be viewed as a special case of that of transfer reactions, which are discussed in the following subsection.

3.7. Reactions with the exchange of several nucleons

These are reactions of the type $A(a,b)B$ in which protons and/or neutrons are exchanged between the target nucleus and the bombarding ion, leading to the production of nuclei b and B in the exit channel. This transfer can occur in several stages (sequential transfer).

The information on light exotic nuclei obtained from such reactions by the end of the 1980s has been reviewed in detail in Ref. 25. Up to now these reactions have been used in the belief that they are a very effective method of studying exotic nuclei. With the transfer of 3–5 nucleons it becomes possible to reach the neutron drip line for nuclei with mass number $A \leqslant 16$ and even to find unbound nuclei beyond this line in the form of resonances. For example, during the last few years transfer reactions and ^{13}C and ^{14}C beams have been used at the VICKSI accelerator complex in Berlin to

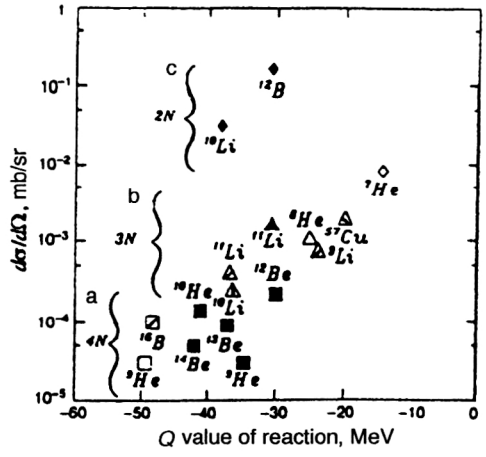

FIG. 12. Systematics of the cross sections for few-nucleon transfer reactions as a function of the Q value of the reaction [Ref. 145]: □ (^{13}C, ^{13}O); ■ (^{14}C, ^{14}O); ⊠ (^{14}C, ^{12}N); △ (^{13}C, ^{14}O); ▲ (^{13}C, ^{12}N); ◬ (^{14}C, ^{17}F); ▲ (^{14}C, ^{13}N); ◬ (^{14}N, ^{15}C); ♦ (^{12}C, ^{12}N); ◇ (^{13}C, ^{15}O).

study the nuclei ^{7,8,9,10}He, ^{10,11}Li, ^{13,14}Be, and ^{14,15,16}B (Refs. 13, 44, 45, 145, 146, and 148–151). At the U-400 accelerator of the Laboratory for Nuclear Research in Dubna and at the NSCL accelerator in Michigan, ^{11}B beams have been used to study the nuclei ^{11}Li and ^{13}Be (Refs. 48 and 147).

The cross sections for few-nucleon transfer reactions with final exotic nuclei in the ground state can be very small. They range from several nanobarns to microbarns. It is very difficult to estimate the cross sections for nuclear fusion near the nucleon stability line. However, on the basis of the data in the literature it can be stated that the yield of such nuclei depends on many factors, such as the number of transferred nucleons, the Q values of the reaction, the structure of the nuclei involved in the reaction, the detection angle, and the energy of the bombarding heavy ion. It has been shown that in principle the cross sections for transfer reactions are large only when certain conditions are satisfied.[152,153] These conditions are related to momentum and angular-momentum conservation in the initial and final nuclei and are stated as

$$\Delta k = k_0 - \lambda_1/R_1 - \lambda_2/R_2 \approx 0, \tag{3.2}$$

$$\Delta L = \lambda_2 - \lambda_1 + 1/2k_0(R_1 - R_2) + QR/(\hbar v) \approx 0, \tag{3.3}$$

where $k_0 = mv/\hbar$, $R = R_1 + R_2$, and v is the relative velocity of the two interacting nuclei in the transfer region. The third condition is that $\ell_1 + \lambda_1$ be even and $\ell_2 + \lambda_2$ be odd. Any deviation from these conditions tends to decrease the cross section for transfer reactions.

The mechanism for the transfer of 1, 2, 3, and more nucleons has been studied in detail in Ref. 154.

The systematics of the cross sections for nucleus production in the ground state in reactions with the transfer of various numbers of nucleons has been constructed as a function of the Q value of the reaction in Ref. 145 (see Fig. 12). The systematics is based on the results of measuring the cross sections for ^{12,13,14}C and ^{14}N beams at energies of 24–30 MeV/A and targets of ^{9,10}Be and ^{13,14}C. We see from Fig. 12 that the cross sections for the transfer of various numbers of nucleons are correlated with the Q value of the

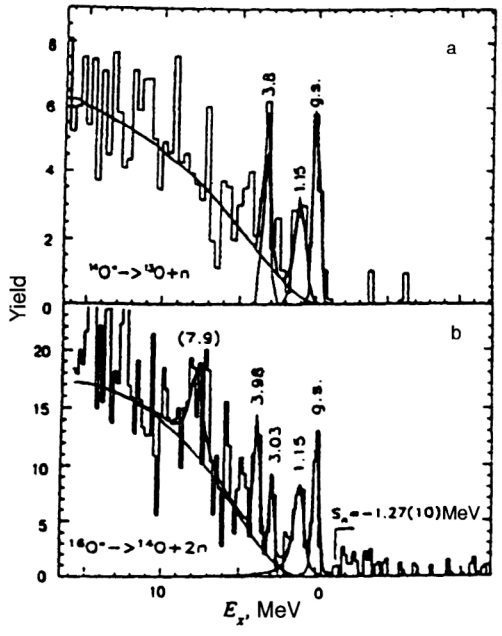

FIG. 13. Energy spectra measured in the reactions ^{9}Be(^{13}C,^{13}O)^{9}He (upper figure) and ^{9}Be(^{14}C,^{14}O)^{9}He (lower figure).[144,145] The upper figure (a) is for 381 MeV at 2.5°, and the lower figure (b) is for 337 MeV at 4.6°–6.4°.

reaction. For example, a 10-fold increase of the cross section is observed when the Q value is 30–40 MeV larger in 4-nucleon transfer (Fig. 12a), when it is 20–30 MeV larger in 3-nucleon transfer (Fig. 12b), and when it is 15–20 MeV larger in 2-nucleon transfer (Fig. 12c). Thus, on the average there is a 10-fold gain in the cross section for isotope production when the Q value of the reaction is more positive by 10 MeV/(transferred nucleon). Nevertheless, it follows from Fig. 12 that in some cases it is more advantageous to use a reaction in which a smaller number of nucleons is transferred instead of a reaction with a more negative value of Q.

The mechanism of transfer reactions is discussed in more detail in the following section.

4. TRANSFER REACTIONS FOR SPECTROSCOPIC STUDIES OF LIGHT EXOTIC NUCLEI

In this section we describe reactions involving proton capture and neutron stripping. Examples of such reactions are charge-exchange reactions such as (^{13}C, ^{13}O) and (^{14}C, ^{14}O) leading to ^{9}He production (Fig. 13) in the transfer of four nucleons, two protons and two neutrons. For bombarding ion energies of <35 MeV/A, the contribution of direct charge exchange owing to the NN interaction is

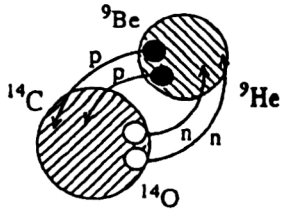

FIG. 14. Transfer mechanism in the double charge-exchange reaction ^{9}Be(^{14}C,^{14}O)^{9}He.

TABLE II. Experimental results for the reaction ^{9}Be(^{13}C, ^{13}O)^{9}He at the angle 2.5° (Ref. 144).

E_x [MeV]	E_R [MeV]	Γ_R [MeV]	$d\sigma/d\Omega$ [nb/sr]	Θ_{cm} [deg]
0.00	1.20(8)	0.10(6)	45(15)	6.6
1.15(10)	2.35(10)	0.70(10)	35(20)	6.6
3.80(12)	5.00(12)	0.20(10)	30(20)	6.7

insignificant.[155] These reactions can therefore be viewed as two-stage processes with effective spectroscopic amplitudes.[156] Figure 14 illustrates the transfer mechanism in the ^{9}Be(^{14}C, ^{14}O)^{9}He reaction: two neutrons are transferred to the target by the bombarding ion (first stage) and two protons are transferred in the opposite direction (second stage) or vice versa.

As a result, for the ^{9}Be(^{14}C, ^{14}O)^{9}He reaction we have the following processes (first stage 1, then stage 2):

$(2n2p)$: ^{9}Be(^{14}C, ^{12}C)^{11}Be(^{12}C, ^{14}O)^{9}He

$(2p2n)$: ^{9}Be(^{14}C, ^{16}O)^{7}He(^{16}O, ^{14}O)^{9}He,

or for the ^{9}Be(^{13}C, ^{13}O)^{9}He reaction:

$(2n2p)$: ^{9}Be(^{13}C, ^{11}C)^{11}Be(^{11}C, ^{13}O)^{9}He

$(2p2n)$: ^{9}Be(^{13}C, ^{15}O)^{7}He(^{15}O, ^{13}O)^{9}He.

The cross section for ^{9}He production is equal to the coherent sum of the $(2n2p)$- and $(2p2n)$-transfer amplitudes. The spectroscopic information obtained for ^{9}He in the reaction ^{9}Be(^{13}C, ^{13}O)^{9}He is given in Table II. The cross sections for this reaction were measured at the angle $\Theta_{lab} = 2.5°$ and amount to 30–50 nb/sr (Ref. 144). The two-stage mechanism describing these cross sections includes the transitions indicated in Fig. 15. In this case the intermediate reaction channels are ^{11}C+^{11}Be and ^{15}O+^{7}He. Pairs of neu-

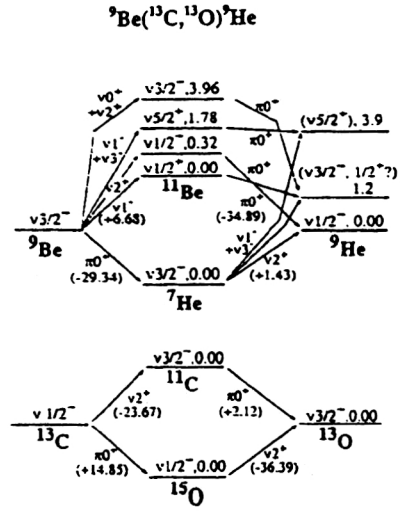

FIG. 15. Transitions to various levels of the ^{9}He nucleus occurring in the reaction ^{9}Be(^{13}C,^{13}O)^{9}He. The change of binding energy is given in parentheses. The spin transfers are also indicated. Two-stage mechanism for transitions in the target nucleus (upper figure) and for transitions in the bombarding ion (lower figure). The distances between levels are shown schematically.

trons and protons are treated as clusters with spin 0^+. Nucleon exchange occurs via neutron and proton transitions in both the bombarding nucleus and the target nucleus. These transitions have the following spectroscopic amplitudes [bound states are denoted as $\phi_{nlj}(2n)$ and $\phi_{nlj}(2p)$, and states in the final nucleus as J^π]:

$(2n2p)$, bombarding ion:

$$A^{\text{proj}}_{2\nu 2\pi}({}^{13}\text{C}_{1/2^-}\rightarrow{}^{13}\text{O}_{3/2^-})\sim A^{\text{proj}}_{2\nu}({}^{11}\text{C}_{3/2^-},\phi^{\text{proj}}_{nlj}(2n)|{}^{13}\text{C}_{1/2^-})\otimes A^{\text{proj}}_{2\pi}({}^{11}\text{C}_{3/2^-},\phi^{\text{proj}}_{nlj}(2p)|{}^{13}\text{O}_{3/2^-});$$

$(2n2p)$, target:

$$A^{\text{targ}}_{2\nu 2\pi}({}^{9}\text{Be}_{3/2^-}\rightarrow{}^{9}\text{He}_{J^\pi})\sim A^{\text{targ}}_{2\nu}({}^{9}\text{Be}_{3/2^-},\phi^{\text{targ}}_{nlj}(2n)|{}^{11}\text{Be}_{J^\pi})\otimes A^{\text{targ}}_{2\pi}({}^{9}\text{He}_{J^\pi},\phi^{\text{targ}}_{nlj}(2p)|{}^{11}\text{Be}_{J^\pi});$$

$(2p2n)$, bombarding ion:

$$A^{\text{proj}}_{2\pi 2\nu}({}^{13}\text{C}_{1/2^-}\rightarrow{}^{13}\text{O}_{3/2^-})\sim A^{\text{proj}}_{2\pi}({}^{13}\text{C}_{1/2^-},\phi^{\text{proj}}_{nlj}(2p)|{}^{15}\text{O}_{1/2^-})\otimes A^{\text{proj}}_{2\nu}({}^{13}\text{O}_{3/2^-},\phi^{\text{proj}}_{nlj}(2n)|{}^{15}\text{O}_{1/2^-});$$

$(2p2n)$, target:

$$A^{\text{targ}}_{2\pi 2\nu}({}^{9}\text{Be}_{3/2^-}\rightarrow{}^{9}\text{He}_{J^\pi})\sim A^{\text{targ}}_{2\pi}({}^{7}\text{He}_{3/2^-},\phi^{\text{targ}}_{nlj}(2p)|{}^{9}\text{Be}_{3/2^-})\otimes A^{\text{targ}}_{2\nu}({}^{7}\text{He}_{3/2^-},\phi^{\text{targ}}_{nlj}(2n)|{}^{9}\text{He}_{J^\pi}).$$

Transitions only between ground states occur in the bombarding ion (lower part of Fig. 15), because, on the one hand, the ^{13}O nucleus can be detected only in the ground state (its excited states are unbound), and, on the other, higher-order transitions via excited states of ^{11}C and ^{15}O are unlikely.[156]

The situation regarding transitions in the target nucleus is somewhat different, as can be seen from Fig. 15 (upper part): ${}^{9}\text{Be}_{3/2^-}\rightarrow{}^{9}\text{He}_{J^\pi}$ ($J^\pi=\frac{1}{2}^-$ for the ground state and $\frac{1}{2}^+$, $\frac{5}{2}^+$, and $\frac{3}{2}^-$ for excited states). Low-lying levels of ^{9}He are formed exclusively by neutron excitations, since the two protons are very strongly bound in the nucleus (the ^{4}He core). As a result, the ^{9}He levels are populated in the $2n$-transfer stage, independently of whether this is the first or second stage. If it is the first stage, i.e., if the population occurs via ^{11}Be states, then already in the intermediate reaction the characteristics of the ^{9}He levels are predetermined. This can be seen from Fig. 15, where the arrows connect the ^{11}Be levels to the ^{9}He levels with the same spins and parities. The stripping of $2p$ in the second stage, with $\pi 0^+$, does not change the J^π of the configuration. This fact can be used to identify the spin and parity of the ^{9}He levels by comparing the probabilities for populating them with the probabilities for populating known states in ^{11}Be. When ^{9}He levels are populated via ^{7}He, the neutron pair (in the second stage) is transferred to the corresponding orbits.

The concept of a semiempirical calculation of the ^{9}He level-population probabilities was developed in Ref. 156. It follows from the above discussion that 2-neutron transfer in either the first or the second stage populates the same J^π configurations with roughly identical spectroscopic amplitudes. The same can be said of 2-proton transfer. The transition probability in second order is therefore proportional to $A^{\text{targ}}_{2\nu}\times A^{\text{targ}}_{2\pi}$ for transitions in the target nucleus in the case

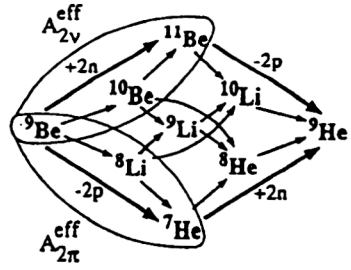

FIG. 16. Multistage contributions for transitions in the target nucleus leading to the ^{9}He nucleus. The contributions to the effective spectroscopic amplitudes of the first stage, $A^{\text{eff}}_{2\nu}$ and $A^{\text{eff}}_{2\pi}$, are circled.

where both amplitudes $(2n2p)$, $(2p2n)$ are two-stage ones, and proportional to $A^{\text{proj}}_{2\nu}\times A^{\text{proj}}_{2\pi}$ for transitions in the bombarding ion. In this approximation the experimentally determined spectroscopic amplitude of the first stage for, for example, $(2n2p)$ transfer can also be used in the second two-stage $(2p2n)$ process as the spectroscopic amplitude of the second stage. Then the differential cross section $d\sigma/d\Omega$ is proportional to $[(A^{\text{targ}}_{2\nu}\times A^{\text{proj}}_{2\nu})\times(A^{\text{targ}}_{2\pi}\times A^{\text{proj}}_{2\pi})]^2=[A_{2\nu}\times A_{2\pi}]$.

In addition to 2-stage processes, we can include the contribution from 3- and 4-stage processes, with individual nucleons transferred in, for example, the following steps:

$$^{9}\text{Be}(^{13}\text{C},\ ^{12}\text{C})^{10}\text{Be}(^{12}\text{C},\ ^{11}\text{C})^{11}\text{Be}(^{11}\text{C},\ ^{13}\text{O})^{9}\text{He}$$

or

$$^{9}\text{Be}(^{13}\text{C},\ ^{14}\text{N})^{8}\text{Li}(^{14}\text{N},\ ^{15}\text{O})^{7}\text{He}(^{15}\text{O},\ ^{13}\text{O})^{9}\text{He}.$$

In this case, as shown in Fig. 16, in addition to two 2-stage amplitudes there are also six 3-stage and six 4-stage amplitudes. However, the contribution of these processes makes up a small part of the total cross section. It can be assumed that the measured spectroscopic amplitudes for neutron and proton pairs actually include higher-order amplitudes, such as the transfer of individual nucleons and inelastic scattering. Therefore, the product of spectroscopic amplitudes obtained experimentally is the effective spectroscopic amplitude, $A^{\text{eff}}_{2\nu}=A^{\text{eff,targ}}_{2\nu}\times A^{\text{eff,proj}}_{2\nu}$ (and analogously for $A^{\text{eff}}_{2\pi}$).

By using the same effective spectroscopic amplitudes $A^{\text{eff}}_{2\nu}$ and $A^{\text{eff}}_{2\pi}$ in the first and second transfer stages (Fig. 16), we have already included four of the six 3-stage and two of the six 4-stage amplitudes. This concept of effective spectroscopic amplitudes has been used to describe the cross sections and angular distributions obtained in experiments on the spectroscopy of ^{8,9,10}He.

Two-stage calculations were performed using the FRESCO program[157] for the coupled-channel model with the same values of A^{eff} for the first and second stages. The cross sections for the reactions corresponding to the first stage of the ^{9}He(^{13}C, ^{13}O)^{9}He reaction were measured experimentally. The spectra are shown in Fig. 17. Here we also indicate the spins and parities of the ^{11}Be levels. The angular distributions of the state $^{11}\text{Be}(\frac{1}{2}^-)$ and the $^7\text{He}(\frac{3}{2}^-)$ ground state were also measured (see Fig. 18). The values of $A^{\text{eff}}_{2\pi}$ and $A^{\text{eff}}_{2\nu}$

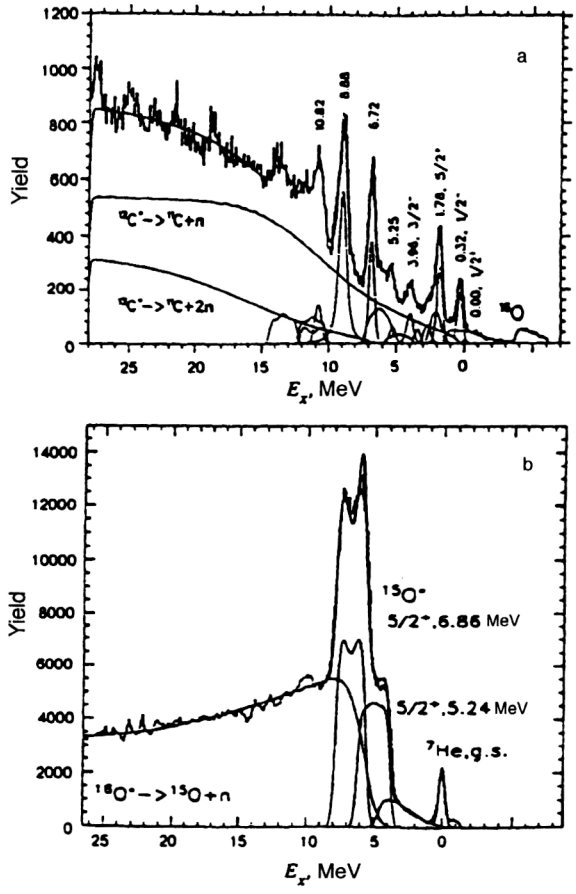

FIG. 17. Energy spectra measured in the reaction ^{9}Be(^{13}C,^{11}C)^{11}Be (upper figure) and the reaction ^{9}Be(^{13}C,^{15}O)^{7}He (lower figure).[156] The upper figure (a) is for 379 MeV at 6°, and the lower figure (b) is for 337 MeV at 2.5°.

were determined by comparing the calculated and experimental cross sections for populating the ground state of ^{7}He and levels of ^{11}Be, respectively (Table III).

The results of the calculations for the ^{9}He(^{13}C, ^{13}O)^{9}He reaction are shown in Fig. 18. In the upper parts of the figures for the $\frac{1}{2}^-$ and $\frac{5}{2}^+$ levels we give the experimental cross sections for intermediate reaction channels (dark symbols for ^{11}Be and light ones for ^{7}He) together with the calculated values (the line with long dashes for $2n$ stripping and the dot–dash line for $2p$ capture). In the lower parts of the figures we show the calculated coherent sum of the $2n2p$- and $2p2n$-exchange amplitudes (solid line). We see that the 2-stage calculations of the level-population cross sections agree within the errors with those measured experimentally without additional normalization.

The good agreement allowed the use of this method for calculating the angular distribution of the first excited state of ^{9}He, which is assigned the values $J^\pi=\frac{1}{2}^+$ or $\frac{3}{2}^-$. The corresponding level-population cross sections for ^{11}Be and ^{9}He are shown in the lower part of Fig. 18. Better agreement between the calculated and experimental values is obtained for $J^\pi=\frac{3}{2}^-$. This value is also consistent with the measured width of the resonance with $E^*=1.15$ MeV, equal to $\Gamma=0.7(1)$ MeV, because the R-matrix calculation gives $\Gamma=0.7-0.8$ MeV for $J^\pi=\frac{3}{2}^-$ and $\Gamma=1.5-2.0$ MeV for $J^\pi=\frac{1}{2}^+$.

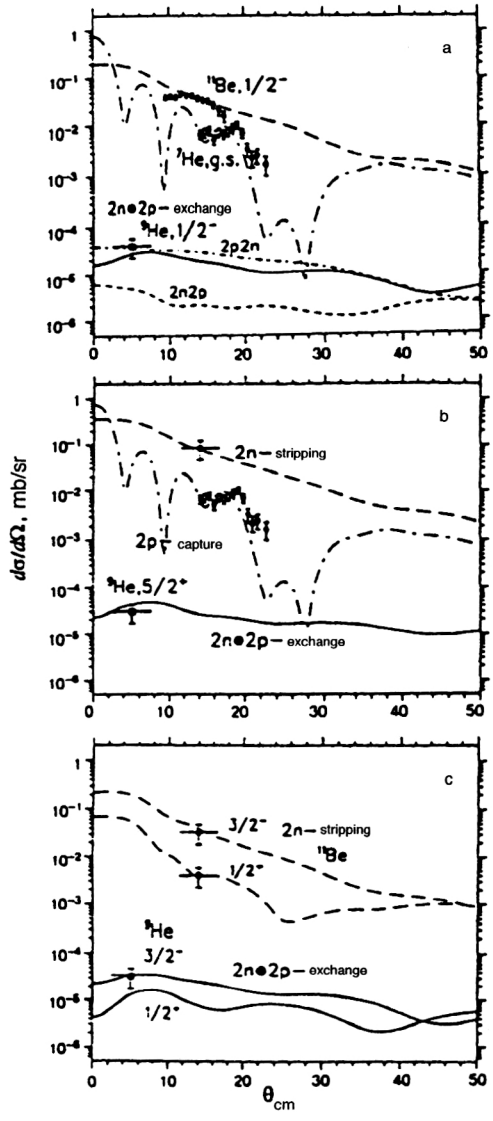

FIG. 18. Comparison of two-stage calculations with the experimental data on the cross sections for level population in the ^{9}He nucleus: for the $\frac{1}{2}^-$ ground state (upper part), for the $\frac{5}{2}^+$ state (central part), and for the two possibilities, $\frac{1}{2}^+$ and $\frac{3}{2}^-$, for the first excited state (lower part).[156] See the text for more details.

It should be noted that a similar result was also obtained in the calculation for the reaction ^{9}Be(^{14}C, ^{14}O)^{9}He.

We can therefore conclude that the effective spectroscopic amplitudes measured for individual stages can successfully be used to estimate the cross sections of two-stage processes in the case of $2n2p$ exchange. Consequently, by using the measured cross sections for 1- and 2-nucleon transfer reactions we should be able to predict the cross sections for 3- and 4-nucleon transfer in the nb/sr range. This is in fact being done in evaluating the possibilities offered by such experiments.

5. SOME METHODS OF STUDYING THE STRUCTURE OF NEUTRON-RICH NUCLEI

It follows from the above discussion that nucleon transfer reactions are an effective tool for spectroscopic studies of

TABLE III. Experimental values of the spectroscopic amplitudes $A_{2\nu}^{\text{eff}}$ and $A_{2\pi}^{\text{eff}}$ for the ^{9}He nucleus obtained in the reactions ^{9}Be(^{13}C, ^{13}O)^{9}He and ^{9}Be(^{14}C, ^{14}O)^{9}He.

		Transitions in the bombarding ion				
		$A_{2\nu}^{\text{eff}}$		$A_{2\pi}^{\text{eff}}$		
Transitions in the target—neutron stripping		^{13}C–^{11}C	^{14}C–^{12}C	^{13}C–^{15}O	^{14}C–^{16}O	Transitions in the target—proton capture
^{9}Be–^{11}Be	$1/2^-$	1.30	1.50	1.60	0.75	^{9}Be–^{7}He, $3/2^-$
	$1/2^+$	1.10	0.85			
	$5/2^+$	0.65	1.00			
	$3/2^-$	1.20	1.00			

exotic nuclei. In addition to binary reactions, of which transfer reactions form a subclass, other methods are also used in the spectroscopy of nuclear states unstable to nucleon emission. For example, the invariant-mass method, which does not make use of the binary nature of a reaction, has recently been widely applied.

Since later on we will give the results obtained using both methods, here we perform a comparative analysis of them.

5.1. Binary reactions

Nucleon transfer reactions can be described by two-body kinematics. For the reaction $A(a,b)B$ measurement of the energy spectrum of the product b emitted at a particular angle allows information to be extracted about the characteristics of the recoil nucleus B—its mass and excited states, even when B is unstable to nucleon emission and direct detection of B is impossible. Spectrometric information about the nucleus under study is obtained by measuring the energy spectrum of nucleus b, from which the Q value of the reaction is extracted. This spectrum can have a rather complicated structure, and it is very important to take into account all its various components. An example of such a spectrum is shown schematically in Fig. 19. The presence of peaks in this spectrum indicates that the nuclei b and B are produced in certain energy states. In Fig. 19, E_{thr} denotes the threshold at which the emission of one or more nucleons or clusters from nucleus B begins, for example, $E_{\text{thr}}=B_n$ or B_{2n}, and so on. Various situations can arise here.

i. The nucleus B may be nucleon-stable. Then a peak shifted to the right (higher energies) of E_{thr} appears in the energy spectrum of nucleus b. If the detected nucleus b has nucleon-stable excited states, they will also be observed in the spectrum. However, they will be broadened, owing to in-flight γ emission. When b does not have nucleon-stable states, the presence of peaks to the right of E_{thr}, i.e., for $E^*\leqslant E_{\text{thr}}$, implies that the nucleus B has bound excited states.

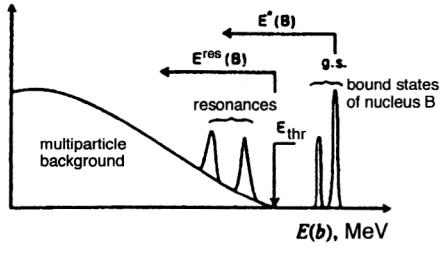

FIG. 19. Schematic representation of the energy spectra obtained in two-body reactions.

ii. The nucleus B may contain states which are unstable to nucleon emission. Then peaks lying to the left (lower energies) of E_{thr} are observed in the spectrum. When there is an unstable state in the nucleus B decaying as $B\rightarrow x+C$, the binary nature of the reaction persists, because the lifetime τ of a resonance in the $(x+C)$ system is larger than the typical reaction time t ($t\leqslant 10^{-22}$ sec). Therefore, in reactions with the transfer of several nucleons it is possible to measure isotope states which exist for a very short time.[45,148] The lifetime τ of a state is extracted from the width Γ of the corresponding peak in the spectrum of the detected particle b. The width of the peak also gives indirect information for identifying the quantum numbers of the levels.

iii. The nucleus B may be unstable in the ground state. In this case peaks with energy below E_{thr} are not observed at all, and the lowest-lying resonance is assumed to correspond to the ground state of nucleus B. It is located to the left of E_{thr} at a distance equal to the energy of the decay with emission of the corresponding number of nucleons, and has width Γ from which the lifetime of B can be determined.

iv. The nucleus B may not exist as a bound system. Then the measured spectrum of b will not contain peaks, but will be smooth.

Let us discuss the nature of the broad distribution below the peaks. In principle, it is a superposition of the contributions of various reactions leading to more than two particles in the exit channel. One of the possible processes is a binary transfer reaction of the type

$$a+A\rightarrow D+E,$$

where $D=(b+x)$ and $E=B-x$. In this case the detected nucleus b is a decay product of the nucleon-unstable excited nucleus D produced in the first stage of the interaction, which decays in-flight into two particles b and x. The shape of the b spectrum is calculated from the decay of the resonance $(b+x)$, lying near the giant dipole resonance. This process can contribute to the final state of the $b+x$ system even during the very short interaction time (of order 10^{-22} sec). Another mechanism occurs when the nucleus B decays into two or more particles. In principle, experiments in which only one product is detected in a reaction involving more than two particles are kinematically incomplete, and

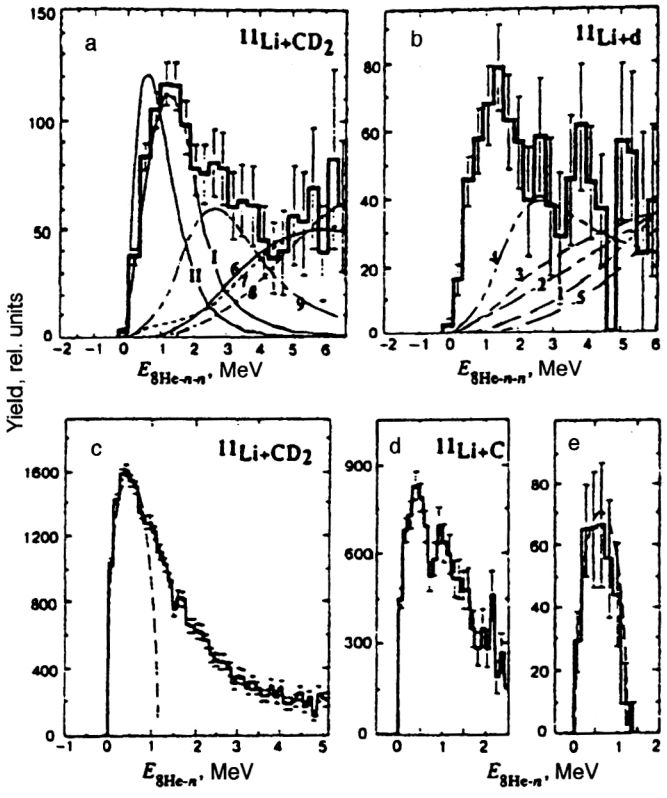

FIG. 20. Invariant-mass spectra of ^{8}He+n+n and ^{8}He+n systems from the reactions (a) $CD_2(^{11}\text{Li}, 2n^8\text{He})$, (b) $d(^{11}\text{Li}, 2n^8\text{He})$, (c) $CD_2(^{11}\text{Li}, n^8\text{He})$, (d) $C(^{11}\text{Li}, n^8\text{He})$, and (e) ^{10}He decay.[43]

these channels are manifested in the energy spectrum of b only as broad, continuous distributions. In the absence of any interaction between the particles in the final state, the continuous spectrum is described by the phase space of these particles. The peaks corresponding to resonances lie on the background produced by processes occurring without the formation of an intermediate state.

Some aspects of the continuum description are discussed in more detail in Ref. 158. Clearly, in analyzing the experimental data for the accurate determination of the peak locations and widths it is important to correctly take into account the various processes contributing to the continuum.

In experiments of this type using transfer reactions it is possible to determine whether or not the nucleus B exists at all as a bound system, to measure its mass and lifetime, and to find excited states.

However, to study the nucleus B in this case it is necessary to select nuclei a, A, and b with well known properties. It is desirable that the nucleus b either not possess nucleon-stable excited states (i.e., that it not possess levels below the threshold for breakup with neutron emission), or that such states lie at excitation energies high enough that they do not interfere with the interpretation of the measured spectrum. In this case the following nuclei are usually used: ^{8}B, ^{9}C, ^{12,13}N, ^{13}O, ^{14}O, ^{17}Ne, and ^{20}Mg. It is also possible to use ^{14}B, ^{10}C, and ^{16}O, whose first excited states are high, and also ^{17}F, whose first bound level has been shown experimentally to be very weakly populated.

5.2. The invariant-mass method

Invariant-mass measurements are also used to search for nucleon resonances in nuclei.

This method for spectroscopic studies does not impose any special requirements on the entrance channel (see, for example, Ref. 43). It is used at high energies in the case of fragmentation of the bombarding ion on a thick target (the invariant mass is defined independently of the beam energy), followed by production of a series of particles $x+C+Y+Z+\ldots$ in the exit channel. The momenta and energies of the particles of any subsystem of two or more particles are measured (for example, $x+C$ in the simplest case if the experiment is designed to obtain information about the nucleus $B=x+C$). The kinematically complete information about the $x+C$ subsystem is used to calculate the invariant mass of B in the c.m. frame of this subsystem. The energy above the breakup threshold for $B\rightarrow x+C$, which corresponds to the decay energy E_{decay}, is equal to the difference between the invariant mass and the sum of the rest masses of particles x and C. If there are resonance states in the nucleus B, they are observed as peaks in the invariant-mass spectrum (Fig. 20).

However, this method has some defects.

First, it is characterized by very small detection efficiency, especially for neutrons, owing to the small angular acceptance of the detectors. High angular resolution is essential. Moreover, the total efficiency depends on the particle energy, owing to the restricted solid angle.

Second, the method is based on the assumption that the detected particles are in the ground state. However, in, for example, the case $B=^{10}\text{Li}=^9\text{Li}+n$ the nucleus $^9\text{Li}=C$ can be formed in the first nucleon-stable excited state with $E^*=2.69$ MeV. This state decays in flight, emitting a γ quantum which is not detected and not taken into account in calculating the invariant mass. Events corresponding to this

case are treated as though their mass were 2.69 MeV closer to threshold. The invariant-mass spectrum is distorted as a result of the superposition of the cross sections for producing the ground and excited states. This problem can be solved in two ways: by measuring the γ quanta or by calculating the Q value for each event, knowing the exact energy of the bombarding ion and using thin targets.

An additional problem in using this method is the presence of decays of resonances in intermediate subsystems with masses greater than that studied in the experiment.

In this rather brief description of the possible ways of obtaining exotic nuclei, our representation of the various nuclear reactions and methods of studying nuclei near the nucleon stability line is not at all complete. We have mentioned only the main reactions and methods which in our opinion can be used successfully at the present time and which give a sensible result. Meanwhile, since the synthesis of new nuclei is a fundamental, many-faceted problem involving not only nuclear physics but also elementary-particle physics, it is natural to use a wide diversity of beams ranging from γ quanta and pions to high-energy heavy ions for solving this problem. For example, an experiment based on the missing-mass method in π^+-meson beams was recently performed at Los Alamos in which information about the structure of several light nuclei ranging from ^{6}H to ^{10}Li was obtained.[159] Several years ago at GSI in Darmstadt a new method was used to synthesize nuclei in the fission of uranium nuclei excited at the giant resonance in the interaction of 300 MeV/A uranium nuclei with lead nuclei.[160] In these experiments, among other new nuclei, the doubly magic ^{78}Ni nucleus was found; it had long eluded attempts to discover it in other experiments.

Here we again note that in our opinion the missing-mass method is very promising for the study of the properties of very neutron-rich nuclei of the lightest elements. We have discussed this method above for the case of binary reactions. It can also be applied to three-body reactions. In this case a reaction is selected such that two magic nuclei are produced in the exit channel (for example, ^{4}He and ^{56}Ni, or ^{40}Ca and ^{20}Ne), while the third nucleus is the desired one. For example, in the reaction $^{68}\mathrm{Zn}+^{18}\mathrm{O}\rightarrow^{26}\mathrm{O}+^{56}\mathrm{Ni}+^4\mathrm{He}$ (or $^{68}\mathrm{Zn}+^{18}\mathrm{O}\rightarrow^{26}\mathrm{O}+^{40}\mathrm{Ca}+^{20}\mathrm{Ne}$) it is possible, by measuring the energy spectrum of ^{4}He in coincidence with ^{56}Ni (or the spectrum of ^{40}Ca in coincidence with ^{20}Ne), to determine the mass and excited levels in the ^{26}O system. The application of this method to beams of radioactive nuclei is very promising.

6. STUDY OF THE STRUCTURE OF LIGHT NUCLEI IN REACTIONS USING RADIOACTIVE BEAMS

During the last ten years a new approach to the study of the properties of light nuclei associated with the use of beams of radioactive nuclei has appeared. It allows the systematic study of the properties of nuclei which are unstable to nucleon emission. This method has been discussed in some detail in recent reviews,[90,161] and so here we will only mention its main features and the possibilities of using it to study the structure of light nuclei. The experiments performed in this area can be divided into two groups: measurement of the properties of accelerated radioactive nuclei and study of the characteristics of their interaction with other nuclei. In the first case the beam of studied nuclei is implanted into some detector and then the decay characteristics of the nuclei of this beam are measured. In the second case the characteristics of nuclear reactions under the influence of beams of exotic nuclei are studied (for example, the interaction cross sections, the fragmentation and electromagnetic dissociation reactions, and also the transverse and longitudinal momentum distributions of the reaction products). In nuclear reactions involving beams of secondary radioactive nuclei it has proved possible to measure the masses, radii, lifetimes, and decay modes of many nuclei, and also to discover manifestations of new features of very neutron- and proton-rich nuclei, like the neutron halo (^{11}Li, ^{14}Be, ^{17}B), the neutron skin (^{6}He, ^{8}He), and the proton halo (^{8}B).

6.1. The nucleon density distributions in exotic nuclei

A large amount of information has been obtained in experiments involving radioactive beams of light nuclei regarding the nuclear radii and nucleon density distributions. The interaction cross section σ_I was measured as the difference between the total reaction cross section σ_R and the elastic interaction cross section σ_E ($\sigma_I=\sigma_R-\sigma_E$) in one of the first experiments using a beam of lithium isotopes.[90] In other words, σ_I was defined as the cross section for reactions in which the number of protons and/or neutrons in the beam nuclei is changed. It was found that the interaction cross section is roughly equal to the reaction cross section, $\sigma_I=\sigma_R$, and this was used to determine the interaction radius: $\sigma_I=\pi[R_I(P)+R_I(T)]^2$, where P and T denote the bombarding particle and the target, respectively. The value of $R_I(P)$ is practically independent of the target. Therefore, $R_I(P)$ is a parameter determining the size of the bombarding nucleus. Subsequent calculations using the Glauber model confirmed that the difference between the reaction cross section and the interaction cross section is less than a few percent, especially at high energies. The radii of light nuclei from hydrogen to neon determined in this manner are shown in Fig. 4. We see that for stable nuclei the dependence of the interaction radius on the nuclear mass is described by $R_I \sim A^{1/3}$. However, for unstable nuclei the radii can differ considerably from the value given by this rule.

The interaction cross section σ_I and the reaction cross section σ_R are usually described by the Glauber model,[162] according to which

$$\sigma_R=2\pi\int_0^\infty (1-T(b))b\,db, \tag{6.1}$$

where $T(b)$ is the transmission coefficient for impact parameter b, which is calculated using the nucleon density distribution and the total NN-interaction cross section:

$$T(b)=\exp\left\{-\sum_{kl}\sigma_{kl}\int\rho^z_{Tk}(s)\rho^z_{Pl}(|\mathbf{b}-\mathbf{s}|)d\mathbf{s}\right\}. \tag{6.2}$$

Here ρ^2_{ik} is the nucleon density distribution integrated along the z axis:

$$\rho_{ik}^{z}=\int_{-\infty}^{\infty}\rho_{ik}(\sqrt{s^2+z^2})dz. \tag{6.3}$$

The index is $i=P$ (particle) or T (target), and σ_{kl} is the total nucleon–nucleon interaction cross section (k and l respectively denote the proton and the neutron). The nucleon density distribution in the nucleus is written as $\rho_{ik}(r)$. This approach works well at energies above 100 MeV/nucleon. The elastic scattering of ^{6}He and ^{8}He nuclei on a proton target at 700 MeV/A was recently studied at GSI in Darmstadt.[163] Analysis of the results according to the Glauber model gave the following values for the radii of the nuclear-matter distributions of these nuclei: 2.30±0.07 and 2.45±0.07 F, respectively.

A different approach is used at lower energies. The reaction cross section is parametrized by surface and volume density distributions:

$$\sigma_R=\pi(R_{\rm vol}+R_{\rm surf})\left[1-\frac{B_c}{E_{cm}}\right], \tag{6.4}$$

where $(R_{\rm vol}+R_{\rm surf})$ is the interaction radius composed of surface and volume parts

$$R_{\rm vol}=r_0(A_P^{1/3}+A_T^{1/3}),$$

$$R_{\rm surf}=r_0\left(a\frac{A_P^{1/3}A_T^{1/3}}{A_P^{1/3}+A_T^{1/3}}-c\right), \tag{6.5}$$

and the Coulomb barrier of the interacting system is

$$B_c=\frac{Z_TZ_Pe^2}{1.3(A_P^{1/3}+A_T^{1/3})}. \tag{6.6}$$

The parameters r_0 and a defined in a wide energy range (from 30 to 2100 MeV/nucleon) are independent of the target–particle combination and of the energy and are 1.1 F and 1.85, respectively. The parameter c varies as a function of energy from 1 (at 20 MeV/nucleon) to 2 (at 160–1000 MeV/nucleon). This simple semiempirical formula gives good agreement with experiment at various energies, although it does not include a possible difference between the proton and neutron densities in the diffuse surface layer. In Fig. 21 we show the dependence of r_0 on the isotopic spin of isobaric nuclei determined in this manner.

Information about the proton and neutron distributions in exotic nuclei is also obtained from the elastic scattering of these particles on target nuclei. Elastic scattering is usually analyzed using the optical model and the coupled-channel method, in which the real and imaginary parts of the optical potential are calculated microscopically. In the standard optical model the potential is taken to have the Woods–Saxon form:

$$U(r)=V_{\rm Coul}(r)-Vf_V(r)-iWf_W(r), \tag{6.7}$$

where

$$f_V(r)=(1+\exp[(r-R_V)/a_V])^{-1}$$

$$f_W(r)=(1+\exp[(r-R_W)/a_W])^{-1}$$

$$R_V=r_VA_T^{1/3},\quad R_W=r_WA_T^{1/3},$$

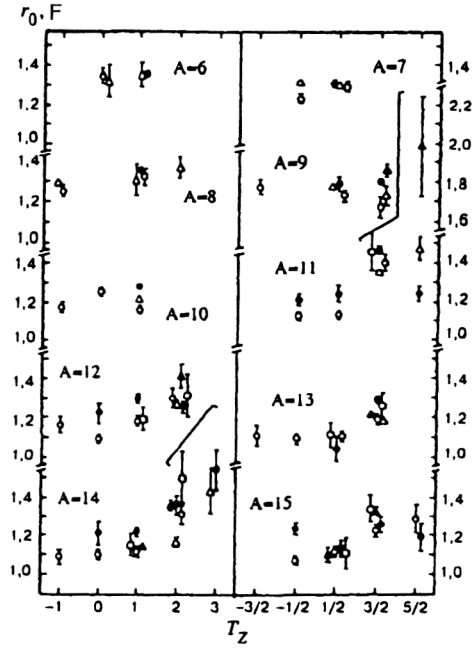

FIG. 21. Comparison of the parameter r_0 obtained in various experiments at energies from 33 MeV/A to 700 MeV/A (Refs. 63 and 64). The parameter r_0 is calculated using Eqs. (6.4)–(6.6).

and $V_{\rm Coul}$ is the Coulomb potential of a uniformly charged sphere. The parameters of the optical model V, W, r_V, r_W, a_V, and a_W are determined by a fit to the experimental data.

The full M3Y interaction with the direct and exchange parts of the potential has recently been used to analyze the elastic scattering of exotic nuclei.[164] In this case the interaction potential is written as a sum: $U(R)=U^D(R)+U^E(R)$, where $U^D(R)$ is the direct potential of the double-folding model. The second term includes the contribution from one-nucleon exchange effects, which can be described using the density-matrix formalism. The iteration method is used to construct the exchange potentials. The number of iterations depends on the energy, the mass numbers of the colliding nuclei, and the distance R. The nucleon density distributions for the particle and target nuclei are calculated by the functional-density method with a single set of parameters. In this case the total potential is taken to be

$$U_t(R)=U(R)+i\left[N_wU(R)-\alpha R\frac{dU(R)}{dR}\right], \tag{6.8}$$

where $U(R)$ includes the direct and exchange parts, and the imaginary term contains the two parameters N_W and α. This representation of the absorption potential makes it possible to avoid the introduction of a phenomenological imaginary part, for example, in the form of a Woods–Saxon potential. On the other hand, the absorption potential has a microscopic origin, and the introduction of the parameter α leads to agreement with the conclusion of multichannel scattering theory that the radius of the absorption potential is larger than the radius of the real part of the potential. The cross sections for elastic scattering calculated for different values of the parameters N_W and α are compared with the experimental results. The approach described above has been used

TABLE IV. Rms radii of the neutron, proton, and matter-density distributions (in F).

Nucleus	$\langle r_n^2\rangle^{1/2}$	$\langle r_p^2\rangle^{1/2}$	$\langle r_m^2\rangle^{1/2}$	δr_{np}
^{7}Be	2.237	2.549	2.420	−0.312
^{8}B	2.190	2.680	2.507	−0.490
^{11}Li	3.255	2.235	3.011	1.020
^{11}C	2.326	2.456	2.398	−0.130
^{12}C	2.387	2.406	2.396	−0.019
^{28}Si	2.953	2.982	2.967	−0.029

successfully to obtain information about the rms radii of the neutron and proton density distributions in nuclei. In Table IV (Ref. 164) we give these values for various nuclei. The microscopic analysis confirms the conclusions drawn earlier in the experiments of Refs. 1, 3, and 65 and in the theoretical studies[89] that a neutron halo exists in ^{11}Li. This is illustrated in Fig. 22, where we show the neutron and proton density distributions in these nuclei. The tail of the neutron distribution in ^{11}Li is clearly expressed. We also see that from the viewpoint of the proton drip line, the tails of the proton densities in ^{8}B and ^{7}Be are significantly higher than the neutron densities, indicating the presence of a proton skin in these nuclei.

Analysis of the data on the elastic scattering of ^{6,7,9,11}Li and ^{4,6,8}He ions on ^{12}C and ^{28}Si targets or on a proton target also required modification of the potential parameters to include the presence of the halo in ^{11}Li and ^{6,8}He (Refs. 79, 80, 165, and 166). The interpretation of the results from the elastic scattering of ^{11}Li and ^{11}C on a ^{12}C target at 60 MeV/A led to a similar conclusion.

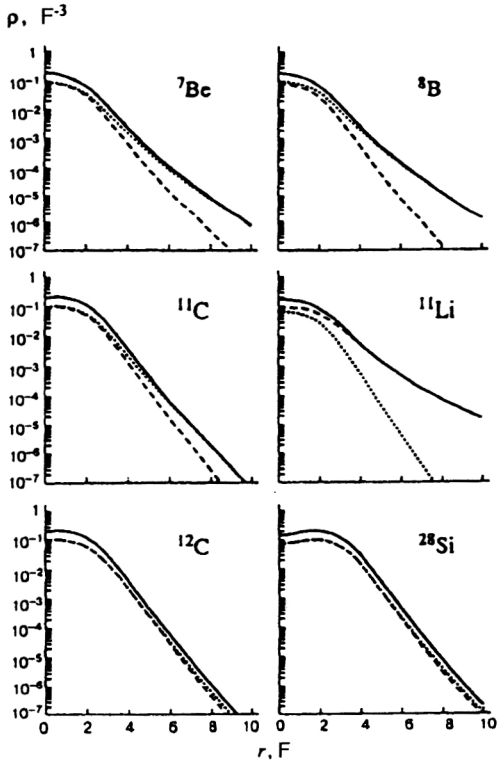

FIG. 22. Density distributions of neutrons (dashed line), protons (dotted line), and matter (solid line) in nuclei.[164]

The valence nucleons of nuclei at the nucleon stability line have extremely small binding energies. For example, in stable nuclei the neutron binding energy is 6–8 MeV, while for very neutron-rich nuclei such as ^{11}Li, ^{11}Be, and ^{14}Be the neutron (or two-neutron) binding energy is several hundred keV. This leads to a broad neutron density distribution in such nuclei (see Fig. 22). The wave function for an outer neutron can be written as

$$\Psi(r)=\left(\frac{2\pi}{k}\right)\frac{e^{-kr}}{r}\left[\frac{e^{kR}}{(1+kR)^{1/2}}\right], \tag{6.9}$$

where R is the width of the potential. Using this wave function, the neutron density distribution can be written as $\rho(r)=|\Psi(r)|^2$. The parameter k determines the slope of the density at the tail of the distribution and is related to the neutron stripping energy E_s: $(\hbar k)^2=2\mu E_s$, where μ is the reduced mass of the system. We see from this expression that when E_s decreases, k becomes small and the tail of the distribution is very extended. As noted above, this leads to the existence of a neutron halo in weakly bound, neutron-rich nuclei.

One method of obtaining information about the neutron halo, including information about the correlations between the neutrons of the halo, is measurement of the momentum distribution of the products—the core and the neutrons of the halo—produced in the fragmentation of nuclei containing a halo (Refs. 4, 28, 29, 65, 70, 71, 77, 78, 81–84, 98, and 167–172).

Practically all nuclei having two-neutron halos are nucleon-stable, while nuclei differing from these by one neutron are nucleon-unstable (nuclei with a two-neutron halo are discussed in Ref. 26). It is therefore obvious that the correlations between the two valence neutrons stabilize nuclei with a halo.

The neutron momentum distribution is given by the Fourier transform of the wave function:

$$f(p)=C/(p_i^2+k^2). \tag{6.10}$$

The width of the momentum distribution depends on the parameter k. In contrast to the density distribution, a decrease of E_s leads to a decrease of the width of the momentum distribution. This is an obvious consequence of the uncertainty principle: when the spatial distribution is broad, the momentum distribution is narrow. Therefore, a neutron halo in nuclei is defined by an extended neutron density distribution and a narrow momentum distribution of the fragmentation products.

In the fragmentation model proposed by Goldhaber,[172] the width of the fragment momentum distribution is described on the basis of the Fermi motion or the temperature corresponding to the binding energy. The model allows an expression to be obtained for the width of the momentum distribution of a fragment of the bombarding ion which depends on the average stripping energy of the outer valence nucleons $\langle\varepsilon\rangle$ and on the masses of the fragment A_F and the bombarding particle A_P:

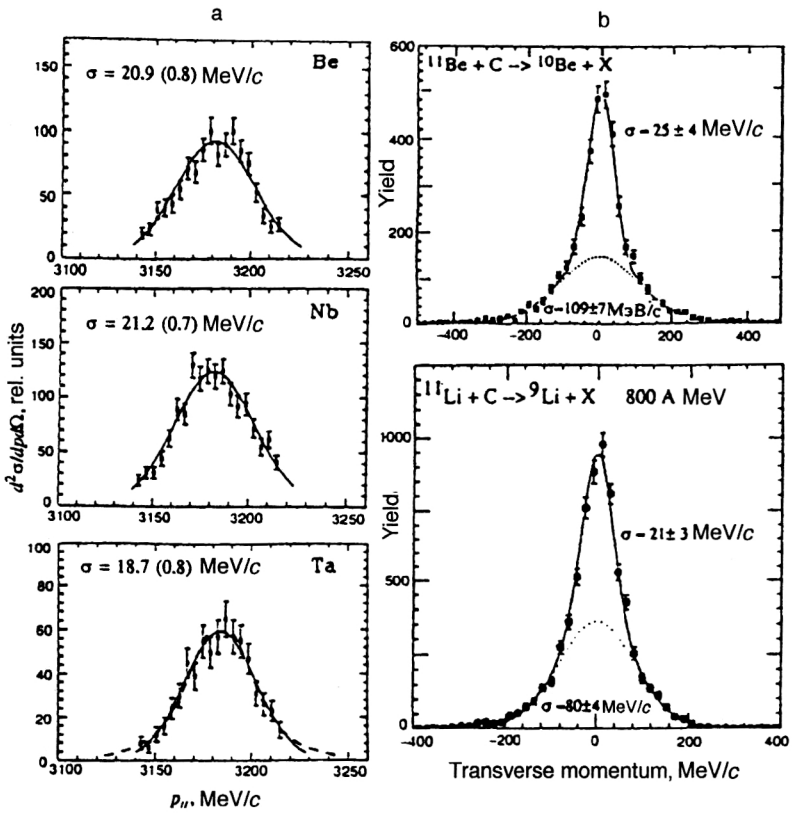

FIG. 23. (a) Longitudinal momentum distributions of ^{9}Li produced in ^{11}Li fragmentation on Be, Nb, and Ta targets and (b) transverse momentum distributions of ^{9}Li and ^{10}Be produced in ^{11}Li and ^{11}Be fragmentation on a C target.[4,77]

$$\sigma^2 = 2u\langle\varepsilon\rangle \frac{A_F(A_P - A_F)}{A_P}, \tag{6.11}$$

where u is the unified mass unit, or

$$\sigma^2 = 2u\langle\varepsilon\rangle \frac{A_P - 1}{A_P}, \tag{6.12}$$

for the stripping of a single nucleon.

The momentum distribution of the heavy fragment of a beam nucleus decaying with the emission of a single nucleon was later analyzed, and it was shown that the momentum distribution of the emitted nucleon at the surface of the beam nucleus can be obtained from the measured fragment momentum distribution. This idea was later extended to the emission of two and more nucleons in the breakup of a beam nucleus.

The first studies to measure the longitudinal momentum of ^{9}Li (Ref. 77) and the angular distribution of an individual neutron[70] in the fragmentation of ^{11}Li did not reveal any dependence on the target nucleus, and so it was concluded that the reaction mechanism is unimportant in the fragmentation of nuclei with a halo. It was therefore decided that the momentum distribution must give direct information about the internal motion of the neutrons in the halo. However, later studies (see, for example, Ref. 81) using ^{11}Be beams showed that the neutron distributions definitely depend on the reaction mechanism, while the longitudinal momentum distribution of the nuclear core does not depend on it. Therefore, the longitudinal momentum distribution of the nuclear core was assumed to be a direct reflection of the ground-state wave function of a nucleus with a halo, i.e., the internal momentum distribution of the nucleons of the halo.

Let us give some examples.

The momentum distributions of fragments produced in ^{11}Li, ^{11}Be, and ^{14}Be fragmentation were measured in Refs. 4, 70, 77, 78, 83, 84, and 167. As an example, in Fig. 23 we show the results for the incident nuclei ^{11}Li and ^{11}Be. We see that the longitudinal momentum distributions of the fragment nuclei ^{9}Li and ^{10}Be respectively produced in the breakup of ^{11}Li and ^{11}Be are very narrow. The transverse momentum distributions have a narrow component superimposed on a broad distribution. According to the uncertainty principle, these narrow widths of order 20–30 MeV/c suggest that the neutrons of the halo have a broad spatial distribution.

Here we should note that the experimental data on the widths of the momentum distributions can be used together with the theoretical expressions to obtain information about the stripping energy of valence neutrons in exotic nuclei.

The fact that the momentum distributions of the fragmentation products are determined not only by the internal motion in the fragmenting nucleus (i.e., by the wave function of the bombarding particle), but also by the reaction mechanism,[167,169] is especially clearly seen from the measured distributions of emitted neutrons.

The neutron distributions in ^{6}He, ^{8}He, ^{9}Li, ^{11}Li, ^{11}Be, and ^{14}Be decay were measured in Refs. 70 and 167. As an example, in Fig. 24 we show the transverse distributions of neutrons from ^{6}He, ^{8}He, ^{9}Li, and ^{11}Li reactions with ^{12}C nuclei. They all have a broad component on which, in the case of nuclei with a halo (^{6}He, ^{8}He, and ^{11}Li) is superimposed a second narrow component. In Ref. 167 (see Fig. 25) this component is associated with the subsequent decay of the nucleus: the first neutron is emitted in the interaction of

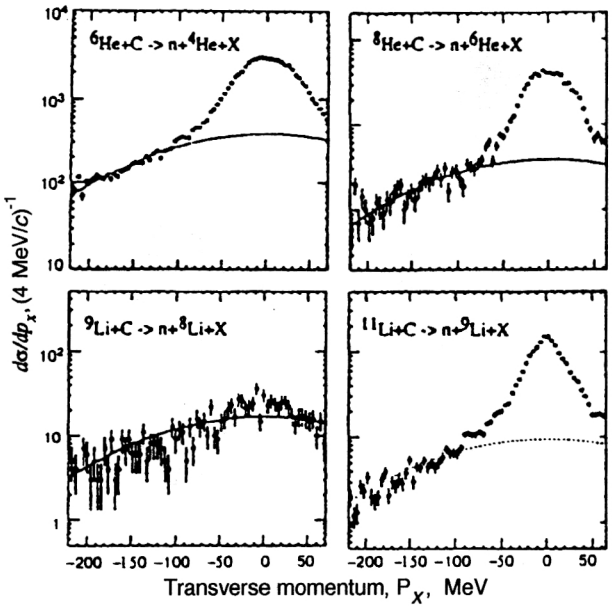

FIG. 24. Transverse-momentum distributions of neutrons in the fragmentation of neutron-rich nuclei at 790 MeV (Ref. 167).

nucleus A with the target, and an unbound intermediate state $(A-1)$ is formed, which then decays by emitting another neutron. In this case the width of the neutron distribution

$$\sigma^2(n)=\frac{2uS_n}{A(A-1)}+\frac{2uQ}{3}\frac{(A-2)}{(A-1)} \tag{6.13}$$

is determined by the decay energy Q of the intermediate state, because the first term is much smaller than the second. The other reaction channels such as direct breakup and sequential decay from excited levels can also have an effect.

At the same time, the width of the heavy-fragment $[(A-2)]$ distribution is given by

$$\sigma(A-2)^2=2M_pS_n\frac{(A-2)^2}{A(A-1)}+2M_pQ\frac{(A-2)}{3(A-1)}, \tag{6.14}$$

where the second term is much smaller. Therefore, $\sigma(A-2)^2$ does not depend on the sequential decay process, but is mainly determined by the fragmentation process and grows smoothly with the energy for stripping one or two neutrons.

Moreover, the widths of the measured transverse distributions of neutrons from ^{11}Be decay become narrower with increasing mass of the target nucleus.[70] This indicates that

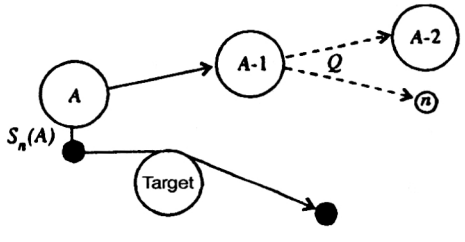

FIG. 25. Graph of sequential decay via an intermediate resonance $(A-1)$.

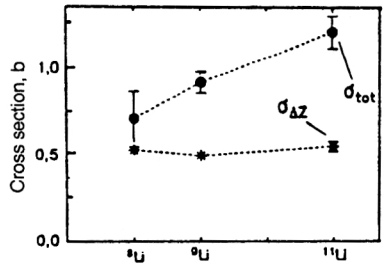

FIG. 26. Cross sections for reactions with changing charge $\sigma_{\Delta Z}$ and total cross sections σ_{tot} in the interaction of ^{11}Li ($E=80$ MeV/A) with a ^{12}C target.[76]

the effect of the Coulomb interaction grows. However, so far there is no definite quantitative conclusion about the relative contributions of the various processes.

It thus appears that the internal motion of the nucleons at the surface of the nucleus must be judged not from the neutron distribution, but from the heavy-fragment momentum distributions.

Another important feature is that the momentum distributions of the decay fragments are narrow only if they result from the stripping of valence neutrons (one or two, depending on the nuclear halo). Otherwise, when many neutrons or protons are stripped off, the widths are larger. This shows that only neutrons in the outer orbit contribute to the halo.

Experiments[75,76] performed using ^{8,9,11}Li beams at 80 MeV/A to determine the total reaction cross sections σ_R and the cross sections for reactions with change of the charge $\sigma_{\Delta Z}$ have shown that the values of $\sigma_{\Delta Z}$ remain practically constant, while σ_R grows with increasing A of the beam (Fig. 26). This indicates that the rms charge radius of all the lithium isotopes is independent of the mass, again confirming that the extended nuclear matter distribution in ^{11}Li is a consequence of the last two weakly bound neutrons.

As already noted, the large increase of the nuclear radius for ^{11}Li, ^{11}Be, ^{14}Be, and ^{17}B (see Fig. 4) and the narrow momentum distribution of the decay fragments indicate the presence of a neutron halo in these nuclei. With the exception of ^{11}Be, all these nuclei have two valence neutrons in the last orbit. All nuclei with a neutron halo have a strongly expressed three-particle configuration, including two weakly bound neutrons and a strongly bound core. The relation between the wave function and the binding energy in this case is much more complicated than in the case of nuclei with a one-neutron halo. Many calculations have been carried out for nuclei with a halo which include the three-particle interaction.

The microscopic three-particle approach, which also includes the neutron interaction with the core, gives the most correct description of the correlations. An example of such a calculation is that of Ref. 89. The results for the ^{6}He nucleus are shown in Fig. 27. There we also compare the distribution in the transverse momentum $p_\perp$ for the ^{4}He nucleus from ^{6}He fragmentation with the three-particle calculation. We see that there is good agreement between experiment and the calculation. Two peaks are observed in the two-neutron densities: one corresponds to the cigar shape, and the other to the dineutron configuration. Actually, the ^{6}He nucleus can

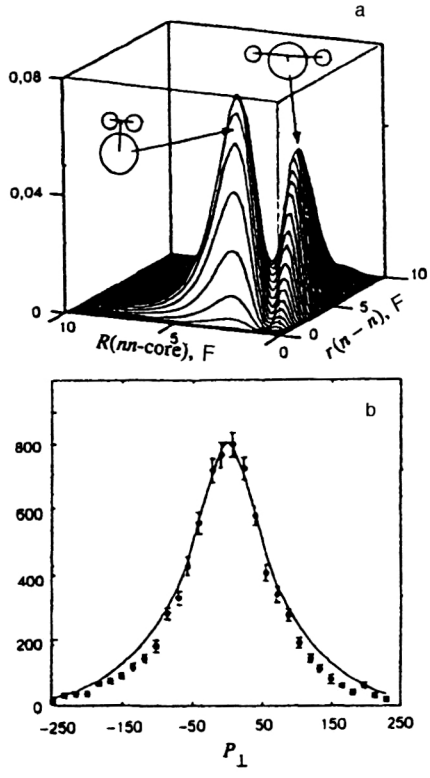

FIG. 27. Three-particle calculation of the two-neutron spatial distribution in the ^{6}He wave function (a) and the ^{4}He momentum distribution (b) in the same calculation.[89]

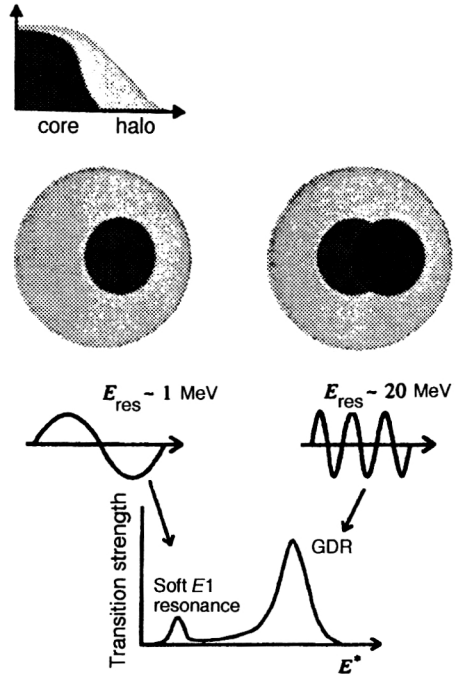

FIG. 28. Schematic representation of the two components of the dipole resonance in neutron-rich nuclei with a halo.

contain a mixture of these two states, but this has not yet been confirmed experimentally.

In addition, fusion reactions followed by fission in ^{6}He beams[174] have shown that the fission cross section is considerably larger than for the ^{4}He nucleus. This increase depends on the entrance channel and is associated with the neutron skin of ^{6}He.

Finally, experiments using secondary beams have allowed the study of the electromagnetic dissociation of exotic nuclei. The predicted[6,174] large value of the cross section for electromagnetic dissociation of ^{11}Li nuclei has been confirmed by experiments at various energies.[5,28,70,75,94] A similar result has also been obtained for ^{11}Be (Refs. 70 and 95) and ^{6,8}He (Ref. 88). A new type of collective excitation at low excitation energies has been suggested to explain the increased Coulomb-dissociation cross section (see Refs. 5, 92, and 93 and references therein). This new excitation mode is referred to as the soft dipole resonance.

6.2. The soft *E*1 excitation mode

It has been suggested that the giant dipole resonance can have two components. One is the result of oscillations of all the protons of the core relative to all the neutrons of the core. The other is the result of oscillation of the entire core relative to the neutrons of the halo. These two processes are shown schematically in Fig. 28. The amplitude of the oscillations, which are referred to as the soft giant-dipole resonance (GDR) mode, is determined by the nucleon density distribution and is proportional to the gradient of the density distribution, and so the oscillation frequency must be very small. The excitation energy is therefore expected to be low, in contrast to the usual giant resonance, where the excitation energy is of order 20 MeV. The existence of the low-energy $E1$ dipole mode has now been confirmed experimentally,[28,82,94,95] but the nature of the excitation mechanism remains in dispute: experiments[82,95,175] indicate that collective excitation does not exist and rule out the presence of a two-neutron halo in the form of a dineutron. However, several theoretical studies[99,176] assume the direct breakup of a nucleus with a halo. The soft dipole resonance must therefore be manifested in the structure of nuclei with a halo either as a low-lying dipole level, or as a strong increase of the reaction cross section near threshold in direct breakup.

The energy of soft GDR modes can be determined using the usual models for describing the GDR. The GDR with the usual excitation energy contributes to the cross section for electromagnetic dissociation σ_{EMD}, but for light exotic nuclei about 10% of the total $E1$ transition probability can be attributed to the soft dipole resonance. The $E1$ transition probability is proportional to the square of the number of neutrons participating in the excitation. Therefore, for ^{11}Li the ratio of the contributions of the soft dipole resonance mode and the ordinary mode is $2^2:6^2$. In this case the energy $E_{\text{soft GDR}}$ must be $0.9^{+0.5}_{-0.3}$ MeV in order to reproduce the observed cross section $\sigma_{EMD}(^{11}\text{Li+Pb})$. The energy $E_{\text{soft GDR}}$ is insensitive to $\Gamma_{\text{soft GDR}}$. Therefore, the excitation energy of the soft dipole resonance is quite small.

Experimental confirmation of the presence of the soft dipole resonance mode has been obtained for ^{11}Li in Ref. 28, where, using the reaction of double charge exchange with pions [^{11}B(π^-,π^+)^{11}Li], it was possible to observe the level $E^* = 1.2 \pm 0.1$ MeV in the pion spectrum and assign it the

spin and parity $\frac{1}{2}^+$, $\frac{3}{2}^+$, or $\frac{5}{2}^+$, from which it was concluded that the $E1$ transition had been observed. However, we think that this result is ambiguous, because collective states are weakly excited in charge-exchange reactions.

Experiments to determine the existence and nature of the soft dipole mode are being carried out by various groups (Michigan, USA; RIKEN, Japan; and JINR, Dubna, Russia).

It has recently been reported,[96] in agreement with the result of an earlier study,[28] that an excited state of the ^{11}Li nucleus at $E^*=1.25$ MeV has been observed in the ^{11}Li $+p$ reaction. This state is assumed to correspond to a halo excitation. The experimental inelastic scattering cross section[97] is described best when it is assumed that orbital angular momentum $L=1$ is transferred, i.e., that there is a dipole excitation.

Here we have touched upon only some of the problems associated with the properties of light nuclei which are being solved by using beams of radioactive nuclei. This area of nuclear physics is developing rapidly. Radioactive beam facilities are being built in several places: SPIRAL in France, the RNB Factory in Japan, the Oak Ridge project in the United States, and so on. The main goal at these centers will be to study the properties and structure of light exotic nuclei. These accelerator complexes of the new generation will produce beams of radioactive nuclei with intensity of up to 10^{11} particles/sec, and will make it possible to perform important, large-scale experiments. In all probability, the work done at these new facilities will represent the next step toward the nucleon stability line for light nuclei. It will result in the synthesis of new nucleon-stable nuclei of light and intermediate elements, which are expected to possess new, unusual states, structural features, and decay modes. Some of the characteristics of exotic nuclei of light elements will be discussed in the second part of this review.

[1] I. Tanihata *et al.*, Phys. Rev. Lett. **55**, 2676 (1985).
[2] I. Tanihata *et al.*, Phys. Lett. B **160**, 380 (1985).
[3] I. Tanihata *et al.*, Phys. Lett. B **206**, 592 (1988).
[4] T. Kobayashi *et al.*, Phys. Rev. Lett. **60**, 2599 (1988).
[5] T. Kobayashi *et al.*, Phys. Lett. B **232**, 51 (1989).
[6] P. G. Hansen and B. Jonson, Europhys. Lett. **4**, 409 (1987).
[7] T. Minamisono *et al.*, Phys. Rev. Lett. **69**, 2058 (1992).
[8] W. Schwab *et al.*, Z. Phys. A **350**, 283 (1995).
[9] C. Detraz and D. J. Vieira, Ann. Rev. Nucl. Part. Sci. **34**, 407 (1989).
[10] T. Motobayashi *et al.*, Phys. Lett. B **346**, 9 (1995).
[11] F. C. Barker and G. T. Hickey, J. Phys. G **2**, L23 (1977).
[12] S. N. Abramovich *et al.*, Yad. Fiz. **46**, 499 (1987) [Sov. J. Nucl. Phys. **46**, 269 (1987)].
[13] H. G. Bohlen *et al.*, Z. Phys. A **344**, 381 (1993).
[14] B. M. Young *et al.*, Phys. Rev. C **44**, 279 (1994).
[15] N. A. F. M. Poppelier *et al.*, Z. Phys. A **346**, 11 (1993).
[16] H. Kitagawa and H. Sagawa, Nucl. Phys. A **551**, 16 (1993).
[17] H. Sagawa *et al.*, Phys. Lett. B **309**, 1 (1993).
[18] A. A. Ogloblin, Z. Phys. A **351**, 355 (1995).
[19] I. Talmi and I. Unna, Phys. Rev. Lett. **4**, 469 (1960).
[20] *Proceedings of the Intern. Symp. on the Structure and Reactions with Unstable Nuclei*, Niigata, Japan, 1991, edited by K. Ikeda and Y. Suzuki (World Scientific, Singapore, 1991).
[21] *Proceedings of the Intern. Conf. on Exotic Nuclei*, Foros, 1991, edited by Yu. E. Penionzhkevich and R. Kalpakchieva (World Scientific, Singapore, 1991).
[22] *Proceedings of the Sixth Intern. Conf. on Nuclei Far from Stability and the Ninth Intern. Conf. on Atomic Masses and Fundamental Constants*, Bernkastel-Kues, Germany, 1992, edited by R. Neugart and A. Wohr (IOP Publishing, Bristol, 1993).
[23] *Proceedings of the Intern. Symp. on the Physics of Unstable Nuclei*, Niigata, Japan, 1994, edited by H. Horiuchi, K. Ikeda, K. Sato *et al.*; Nucl. Phys. A **588** (1995).
[24] *Proceedings of the Intern. Conf. on Exotic Nuclei and Atomic Masses*, Arles, France, 1995, edited by M. de Saint Simon and O. Sorlin (Editions Frontières, 1995).
[25] A. A. Ogloblin and Yu. E. Penionzhkevich, in *Treatise on Heavy Ion Science*, edited by D. A. Bromley (Plenum Press, New York, 1989), Vol. 8, p. 260.
[26] C. A. Bertulani *et al.*, Phys. Rep. **226**, 283 (1993).
[27] A. C. Muller and B. M. Sherrill, Ann. Rev. Nucl. Part. Sci. **43**, 529 (1993).
[28] T. Kobayashi, in *Proceedings of the Intern. Symp. on the Structure and Reactions with Unstable Nuclei*, Niigata, Japan, 1991, edited by K. Ikeda and Y. Suzuki (World Scientific, Singapore, 1991), p. 187; Nucl. Phys. A **538**, 343c (1992).
[29] T. Kobayashi, Nucl. Phys. A **553**, 465c (1993).
[30] P. G. Hansen, Nucl. Phys. A **553**, 89c (1993).
[31] B. Jonson, Nucl. Phys. A **574**, 151c (1994).
[32] K. Riisager, Rev. Mod. Phys. **66**, 1105 (1994).
[33] P. E. Haustein, Special Editor, At. Data Nucl. Data Tables **39**, 185 (1988).
[34] H. A. Bethe, Ann. Rev. Nucl. Sci. **21**, 93 (1971).
[35] J. D. Bowman *et al.*, Phys. Rev. Lett. **31**, 614 (1973).
[36] J. A. Musser and J. D. Stevenson, Phys. Rev. Lett. **53**, 2544 (1984).
[37] J. D. Stevenson and J. P. Price, Phys. Rev. C **24**, 2102 (1981).
[38] A. G. Artyukh *et al.*, in *Abstracts of Reports Presented at the Twenty-Fifth All-Union Meeting on Nuclear Spectroscopy and Structure of the Atomic Nucleus* [in Russian], 1975 (Nauka, Leningrad), p. 223.
[39] M. Langevin *et al.*, Phys. Lett. B **150**, 71 (1985).
[40] F. Pougheon *et al.*, Europhys. Lett. **2**, 505 (1986).
[41] D. Guillemaud-Mueller *et al.*, Z. Phys. A **332**, 189 (1989).
[42] D. Guillemaud-Mueller *et al.*, Phys. Rev. C **41**, 937 (1990).
[43] A. A. Korsheninnikov *et al.*, Phys. Lett. B **326**, 31 (1994).
[44] A. N. Ostrowski *et al.*, Phys. Lett. B **338**, 13 (1994).
[45] H. G. Bohlen *et al.*, Nucl. Phys. A **583**, 775c (1995).
[46] G. Audi, O. Bersillon, J. Blachot, and A. H. Wapstra, Nucl. Phys. A **624**, 1 (1997).
[47] G. Audi and A. Wapstra, Nucl. Phys. A **565**, 1 (1993).
[48] A. V. Belozyorov *et al.*, JINR Rapid Commun. No. 1(69)-95, 11 (1995).
[49] H. G. Bohlen *et al.*, Nucl. Phys. A **616**, 254c (1997).
[50] A. S. Jensen and K. Riisager, Nucl. Phys. A **537**, 45 (1992).
[51] A. G. Artukh *et al.*, Phys. Lett. B **33**, 407 (1970).
[52] H. Sakurai *et al.*, Phys. Rev. C **54**, R2802 (1996).
[53] H. Sakurai *et al.*, Nucl. Phys. A **616**, 311c (1997).
[54] D. V. Aleksandrov *et al.*, Yad. Fiz. **39**, 513 (1984) [Sov. J. Nucl. Phys. **39**, 323 (1984)].
[55] C. Thibault *et al.*, Phys. Rev. C **12**, 644 (1975).
[56] X. Campi *et al.*, Nucl. Phys. A **251**, 193 (1975).
[57] C. Detraz, in *Proceedings of the Fourth Intern. Conf. on Nuclei Far from Stability*, Helsingor, Denmark, 1981, p. 361.
[58] P. J. Woods *et al.*, Phys. Lett. B **182**, 297 (1986).
[59] L. K. Fifield *et al.*, Nucl. Phys. A **484**, 117 (1988).
[60] O. Tarasov *et al.*, JINR Rapid Commun. No. 5(79)-96, 59 (1996).
[61] E. G. Nadjakov *et al.*, At. Data Nucl. Data Tables **56**, 133 (1994).
[62] S. Gerstenkorn, C. R. Acad. Ser. B **268**, 1636 (1969).
[63] M. G. Saint-Laurent *et al.*, Z. Phys. A **332**, 457 (1989).
[64] A. C. Villari *et al.*, Phys. Lett. B **268**, 345 (1991).
[65] I. Tanihata *et al.*, Phys. Lett. B **287**, 307 (1992).
[66] A. Ozawa *et al.*, Phys. Lett. B **334**, 18 (1994).
[67] A. Ozawa *et al.*, Nucl. Phys. A **583**, 807c (1995).
[68] T. Suzuki *et al.*, Nucl. Phys. A **616**, 286c (1997).
[69] A. Ozawa *et al.*, Nucl. Phys. A **608**, 63 (1996).
[70] R. Anne *et al.*, Phys. Lett. B **250**, 19 (1990).
[71] R. Anne *et al.*, Nucl. Phys. A **575**, 125 (1994).
[72] M. Fukuda *et al.*, Phys. Lett. B **268**, 339 (1991).
[73] S. Shimoura *et al.*, in *Proceedings of the Intern. Symp. on the Structure and Reactions with Unstable Nuclei*, Niigata, Japan, 1991, edited by K. Ikeda and Y. Suzuki (World Scientific, Singapore, 1991), p. 132.
[74] K. Riisager *et al.*, Nucl. Phys. A **540**, 365 (1992).
[75] B. Blank *et al.*, Z. Phys. A **340**, 41 (1991).
[76] B. Blank *et al.*, Z. Phys. A **343**, 375 (1992).
[77] N. A. Orr *et al.*, Phys. Rev. Lett. **69**, 2050 (1992).

[78] N. A. Orr *et al.*, in *Proceedings of the Third Intern. Conf. on Radioactive Nuclear Beams*, East Lansing, Michigan, 1993, edited by D. J. Morrissey (Editions Frontières), pp. 145, 345, 389.
[79] M. Lewitowicz *et al.*, Nucl. Phys. A **562**, 301 (1993).
[80] J. J. Kolata *et al.*, Phys. Rev. Lett. **69**, 2631 (1992).
[81] R. Anne *et al.*, Phys. Lett. B **304**, 55 (1993).
[82] D. Sackett *et al.*, Phys. Rev. C **48**, 118 (1993); K. Ieki *et al.*, Phys. Rev. Lett. **70**, 730 (1993).
[83] M. Zahar *et al.*, Phys. Rev. C **48**, R1484 (1993).
[84] J. H. Kelley *et al.*, Phys. Rev. Lett. **74**, 30 (1995).
[85] A. A. Ogloblin, in *Proceedings of the Intern. Conf. on Exotic Nuclei*, Foros, 1991, edited by Yu. E. Penionzhkevich and R. Kalpakchieva (World Scientific, Singapore, 1991), p. 36.
[86] I. Tanihata *et al.*, in *Proceedings of the Sixth Intern. Conf. on Nuclei Far from Stability and the Ninth Intern. Conf. on Atomic Masses and Fundamental Constants*, Bernkastel-Kues, Germany, 1992, edited by R. Neugart and A. Wohr (IOP Publishing, Bristol, 1993), p. 167; Phys. Lett. B **289**, 261 (1992).
[87] S. Neumaier *et al.*, Preprint GSI-94-43, GSI, Darmstadt (1994).
[88] I. Tanihata, Nucl. Phys. A **522**, 275c (1991).
[89] M. V. Zhukov *et al.*, Phys. Rep. **231**, 151 (1993).
[90] I. Tanihata, Prog. Part. Nucl. Phys. **35**, 505 (1995).
[91] I. Tanihata, J. Phys. G **22**, 157 (1996).
[92] K. Ikeda, Nucl. Phys. A **538**, 355c (1992) and references therein.
[93] T. Kobayashi, Preprint 89-148, KEK, Japan (1989) and references therein.
[94] S. Shimoura *et al.*, in *Proceedings of the Sixth Intern. Conf. on Nuclei Far from Stability and the Ninth Intern. Conf. on Atomic Masses and Fundamental Constants*, Bernkastel-Kues, Germany, 1992, edited by R. Neugart and A. Wohr (IOP Publishing, Bristol, 1993), p. 271.
[95] T. Nakamura *et al.*, Phys. Lett. B **331**, 296 (1994); in *Proceedings of the Intern. Symp. on the Physics of Unstable Nuclei*, Niigata, Japan, 1994, edited by H. Horiuchi, K. Ikeda, K. Sato *et al.*, Nucl. Phys. A **588**, 81 (1995).
[96] A. A. Korsheninnikov *et al.*, Phys. Rev. C **53**, R537 (1996).
[97] A. A. Korsheninnikov *et al.*, Phys. Rev. Lett. **78**, 2317 (1997).
[98] D. Bazin *et al.*, Phys. Rev. Lett. **74**, 3569 (1995).
[99] T. Otsuka *et al.*, Phys. Rev. Lett. **70**, 1385 (1993); Phys. Rev. C **49**, 2289 (1994).
[100] I. J. Thompson and M. V. Zhukov, Phys. Rev. C **49**, 1904 (1994).
[101] T. Hoshino *et al.*, Nucl. Phys. A **523**, 228 (1991).
[102] S. L. Whetstone, Jr. and T. D. Thomas, Phys. Rev. **154**, 1174 (1967).
[103] V. L. Mikheev *et al.*, Preprint R7-84-614, JINR, Dubna (1984) [in Russian].
[104] S. W. Cosper *et al.*, Phys. Rev. **154**, 1193 (1967).
[105] R. Bayer *et al.*, Czech. J. Phys. **31**, 1273 (1981).
[106] D. B. Aleksandrov *et al.*, Yad. Fiz. **35**, 277 (1982) [Sov. J. Nucl. Phys. **35**, 158 (1982)]; Yad. Fiz. **36**, 1351 (1982) [Sov. J. Nucl. Phys. **36**, 783 (1982)].
[107] P. Armbruster *et al.*, Europhys. Lett. **4**, 793 (1988).
[108] R. Kalpakchieva *et al.*, Yad. Fiz. **26**, 253 (1977) [Sov. J. Nucl. Phys. **26**, 131 (1977)].
[109] M. Rajagopalan and T. D. Thomas, Phys. Rev. C **5**, 1402 (1972).
[110] E. Duek *et al.*, Z. Phys. A **317**, 83 (1984).
[111] M. Sovinski *et al.*, Preprint R7-85-377, JINR, Dubna (1985) [in Russian].
[112] A. M. Poskanzer *et al.*, Phys. Rev. Lett. **17**, 1271 (1966).
[113] T. D. Thomas *et al.*, Phys. Lett. B **27**, 504 (1968).
[114] V. I. Bogatin *et al.*, Yad. Fiz. **32**, 27 (1980) [Sov. J. Nucl. Phys. **32**, 14 (1980)].
[115] O. V. Lozhkin *et al.*, Preprint RI-168, Leningrad (1983) [in Russian].
[116] A. G. Artukh *et al.*, Nucl. Phys. A **137**, 348 (1969); Phys. Lett. B **31**, 129 (1970); Phys. Lett. B **32**, 43 (1970); Nucl. Phys. A **176**, 284 (1971).
[117] V. V. Volkov, Fiz. Élem. Chastits At. Yadra **2**, 285 (1971) [Sov. J. Part. Nucl. **2**, Part 2, 1 (1971)].
[118] P. Auger *et al.*, Z. Phys. A **289**, 255 (1979).
[119] D. Guerreau *et al.*, Z. Phys. A **295**, 105 (1980).
[120] H. Breuer *et al.*, Phys. Rev. C **22**, 2454 (1980).
[121] Ya. Vil'chinski *et al.*, Yad. Fiz. **5**, 942 (1967) [Sov. J. Nucl. Phys. **5**, 672 (1967)].
[122] A. G. Artukh *et al.*, Nucl. Phys. A **160**, 511 (1971).
[123] V. V. Volkov, Phys. Rep. **44**, 93 (1978).
[124] Yu. Ts. Oganesyan *et al.*, Pis'ma Zh. Éksp. Teor. Fiz. **36**, 104 (1982) [JETP Lett. **36**, 129 (1982)].
[125] H. C. Britt and A. R. Quinton, Phys. Rev. **124**, 877 (1961).
[126] C. Borcea *et al.*, Nucl. Phys. A **391**, 520 (1982).
[127] Yu. É. Penionzhkevich *et al.*, Fiz. Élem. Chastits At. Yadra **17**, 165 (1986) [Sov. J. Part. Nucl. **17**, 65 (1986)].
[128] C. Borcea *et al.*, Nucl. Phys. A **415**, 169 (1984).
[129] D. E. Greiner *et al.*, Phys. Rev. Lett. **35**, 152 (1975).
[130] T. J. M. Symons *et al.*, Phys. Rev. Lett. **42**, 40 (1979).
[131] G. D. Westfall *et al.*, Phys. Rev. Lett. **43**, 1859 (1979).
[132] D. Guerreau, J. Phys. (Paris), Colloq. **4–47**, 207 (1986).
[133] D. Guillemaud-Mueller *et al.*, Z. Phys. A **322**, 415 (1985).
[134] K. Seth, in *Proceedings of the Fourth Conf. on Nuclei Far from Stability*, Helsingor, Denmark, 1981, p. 655.
[135] K. Seth, in *Proceedings of the Fifth Conf. on Nuclei Far from Stability*, Rosseau Lake, Ontario, Canada, 1987, edited by I. S. Towner (AIP, New York, 1988), p. 324.
[136] K. Seth *et al.*, Phys. Rev. Lett. **58**, 1930 (1987).
[137] D. M. Drake *et al.*, Phys. Rev. Lett. **45**, 1765 (1980).
[138] C. Brendel *et al.*, in *Proceedings of the Fourth Conf. on Nuclei Far from Stability*, Helsingor, Denmark, 1981, p. 664.
[139] F. Naulin *et al.*, Phys. Rev. C **25**, 1074 (1982).
[140] L. K. Fifield *et al.*, Nucl. Phys. A **385**, 505 (1982).
[141] T. Ichihara, RIKEN Review No. 4, January, 1994, p. 15.
[142] H. G. Bohlen *et al.*, Nucl. Phys. A **488**, 89c (1988).
[143] W. von Oertzen, Nucl. Phys. A **482**, 357c (1988).
[144] H. G. Bohlen, in *Proceedings of the Intern. Symp. on the Structure and Reactions with Unstable Nuclei*, Niigata, Japan, 1991, edited by K. Ikeda and Y. Suzuki (World Scientific, Singapore, 1991), p. 83.
[145] H. G. Bohlen *et al.*, in *Proceedings of the Fifteenth EPS Nucl. Phys. Divisional Conf. on Low Energy Nuclear Dynamics (LEND '95)*, 1995, St. Petersburg, Russia, edited by Yu. Ts. Oganessian, W. von Oertzen, and R. Kalpakchieva (World Scientific, Singapore, 1995), p. 53.
[146] A. N. Ostrowski *et al.*, Z. Phys. A **343**, 489 (1992).
[147] B. M. Young *et al.*, Phys. Rev. Lett. **71**, 4124 (1993).
[148] W. von Oertzen *et al.*, in *Proceedings of the Intern. Symp. on the Physics of Unstable Nuclei*, Niigata, Japan, 1994, edited by H. Horiuchi, K. Ikeda, K. Sato *et al.*, Nucl. Phys. A **588**, (1995), p. 129c.
[149] H. G. Bohlen *et al.*, in *Proceedings of the Sixth Intern. Conf. on Nuclei Far from Stability and the Ninth Intern. Conf. on Atomic Masses and Fundamental Constants*, Bernkastel-Kues, Germany, 1992, edited by R. Neugart and A. Wohr (IOP Publishing, Bristol, 1993), p. 349.
[150] H. G. Bohlen *et al.*, in *Proceedings of the Intern. School-Seminar on Heavy Ion Physics*, Dubna, 1993, edited by Yu. Ts. Oganessian, Yu. E. Penionzhkevich, and R. Kalpakchieva (JINR, Dubna, 1993), p. 17.
[151] H. G. Bohlen *et al.*, Z. Phys. A **351**, 7 (1995).
[152] D. M. Brink, Phys. Lett. B **40**, 37 (1972).
[153] W. von Oertzen, in *CXII Course on Nuclear Collisions from the Mean-Field into the Fragmentation Regime*, 1991, p. 459.
[154] N. Anyas-Weiss *et al.*, Phys. Rep. **12**, 201 (1974).
[155] H. Lenske *et al.*, Phys. Rev. Lett. **62**, 1457 (1989).
[156] H. G. Bohlen, in *Proceedings of the Intern. Symp. on Large-Scale Collective Motion of Atomic Nuclei*, Brolo (Messina), Italy, 1996, edited by G. Giardina and F. Hanappe (World Scientific, Singapore, 1997), p. 47; H. G. Bohlen *et al.*, in *Proceedings of the Eighth Intern. Conf. on Nuclear Reaction Mechanisms*, Varenna, Italy, 1997, edited by E. Gadioli (Univ. Milano Press, Milan, 1997), p. 425.
[157] I. J. Thompson, Comput. Phys. Commun. **7**, 167 (1988).
[158] H. G. Bohlen *et al.*, Z. Phys. A **320**, 237 (1985).
[159] K. Seth, in *Proceedings of the Intern. Conf. on Exotic Nuclei and Atomic Masses*, Arles, France, 1995, edited by M. de Saint Simon and O. Sorlin (Editions Frontières, 1995), p. 109.
[160] M. Bernas *et al.*, Nucl. Phys. A **616**, 352c (1997).
[161] Yu. É. Penionzhkevich, Fiz. Élem. Chastits At. Yadra **25**, 930 (1994) [Sov. J. Part. Nucl. **25**, 394 (1990)].
[162] R. J. Glauber, *Lectures in Theoretical Physics*, Vol. 1 (Interscience, New York, 1959), p. 315.
[163] G. D. Alkhazov *et al.*, Phys. Rev. Lett. **78**, 2313 (1997).
[164] O. M. Knyaz'kov *et al.*, Yad. Fiz. **59**, 1188 (1996) [Phys. At. Nucl. **59**, 1138 (1996)].
[165] A. A. Korsheninnikov *et al.*, Nucl. Phys. A **616**, 189c (1997).
[166] A. A. Korsheninnikov *et al.*, Nucl. Phys. A **617**, 45 (1997).

[167] T. Kobayashi, in *Proceedings of the Third Intern. Conf. on Radioactive Nuclear Beams*, East Lansing, Michigan, 1993, edited by D. J. Morrissey (Editions Frontières), p. 169.
[168] T. Kobayashi, Nucl. Phys. A **616**, 223c (1997).
[169] T. Nilsson *et al.*, Nucl. Phys. A **598**, 418 (1996).
[170] F. Humbert *et al.*, Phys. Lett. B **347**, 198 (1995).
[171] N. Orr *et al.*, Phys. Rev. C **51**, 3116 (1995).
[172] A. Goldhaber, Phys. Lett. B **53**, 306 (1974).
[173] K. Riisager, in *Proceedings of the Third Intern. Conf. on Radioactive Nuclear Beams*, East Lansing, Michigan, 1993, edited by D. J. Morrissey (Editions Frontières), p. 281.
[174] C. Bertulani and G. Baur, Nucl. Phys. A **480**, 615 (1988).
[175] K. Ieki *et al.*, Phys. Rev. C **54**, 1589 (1996).
[176] G. Baur *et al.*, Nucl. Phys. A **550**, 527 (1992).

Translated by Patricia A. Millard